arXiv:cond-mat/9710050v1 [cond-mat.mes-hall] 6 Oct 1997

International Journal of Modern Physics B,
© World Scientific Publishing Company

OPTICS WITH QUANTUM HALL SKYRMIONS

T. PORTENGEN, J. R. CHAPMAN, V. NIKOS NICOPOULOS, and N. F. JOHNSON
Department of Physics, University of Oxford, Parks Road
Oxford, OX1 3PU, United Kingdom

Received February 1, 2008

A novel type of charged excitation, known as a Skyrmion, has recently been discovered in quantum Hall systems with filling factor near $\nu = 1$. A Skyrmion—which can be thought of as a topological twist in the spin density of the electron gas—has the same charge as an electron, but a much larger spin. In this review we present a detailed theoretical investigation of the optical properties of Skyrmions. Our results provide means for the optical detection of Skyrmions using photoluminescence (PL) spectroscopy. We first consider the optical properties of Skyrmions in disordered systems. A calculation of the luminescence energy reveals a special optical signature which allows us to distinguish between Skyrmions and ordinary electrons. Two experiments to measure the optical signature are proposed. We then turn to the optical properties of Skyrmions in pure systems. We show that, just like an ordinary electron, a Skyrmion may bind with a hole to form a Skyrmionic exciton. The Skyrmionic exciton can have a lower energy than the ordinary magnetoexciton. The optical signature of Skyrmions is found to be a robust feature of the PL spectrum in both disordered and pure systems.

1. Introduction

Imagine piercing a sphere with arrows pointing in a direction normal to the surface of the sphere. Then imagine stereographically projecting the surface of the sphere onto a flat plane, keeping the direction of the arrows fixed. The resulting distribution of arrows in the plane is a vector field with a peculiar twist known as a Skyrmion.

Skyrmions were introduced by T. H. R. Skyrme[1] in 1958 as a way of representing the nucleon in terms of the underlying pion field. During the following decades most interest for Skyrmions came from nuclear physicists and particle physicists. That changed a few years ago when S. L. Sondhi, A. Karlhede, S. A. Kivelson, and E. H. Rezayi[2]—building on earlier work by D. H. Lee and C. L. Kane[3]—predicted the existence of Skyrmions in a two-dimensional (2D) electron system subjected to a perpendicular magnetic field of a particular strength. The strength of the magnetic field is such that the filling factor $\nu = 2\pi\ell^2 n_s$ (where $\ell = \sqrt{\hbar c/eB}$ is the magnetic length and n_s is the electron density) is equal to an odd integer ($\nu = 1, 3, 5, \ldots$). Under these conditions the 2D electron system exhibits the well-known (integer) quantum Hall effect. Skyrmions occuring in a 2D electron system subjected to a magnetic field have thus become known as "quantum Hall" Skyrmions.

The first experimental evidence for quantum Hall Skyrmions was obtained by Barrett, Dabbagh, Pfeiffer, West, and Tycko[4]. They used nuclear magnetic resonance (NMR) spectroscopy to measure the Knight shift of ^{71}Ga nuclei located in a n-doped GaAs quantum well. The Knight shift is directly proportional to the spin polarization of the 2D electron gas surrounding the nuclei. Barrett *et al.* observed a precipitous drop of the Knight shift as the filling factor is varied away from $\nu = 1$, indicating that the spin of the charged excitations at $\nu = 1$ is much larger than $\frac{1}{2}$. Evidence for Skyrmions was also obtained by Schmeller, Eisenstein, Pfeiffer, and West[5] using tilted-field magnetotransport measurements, and by Aifer, Goldberg, and Broido[6] using interband optical transmission spectroscopy. Maude *et al.*[7] have determined the spin activation gap at $\nu = 1$ using transport measurements under hydrostatic pressure. They found that a spin activation gap exists even at zero Zeeman energy, in agreement with the theoretical prediction[2] based on Skyrmions.

The past three years have seen an explosion of theoretical work on quantum Hall Skyrmions. Below we briefly summarize some important developments. In their pioneering paper Sondhi *et al.* employed a field-theoretic approach in which it was difficult to include the effect of a nonzero Zeeman energy. A variational Hartree-Fock approach which allows for the inclusion of the Zeeman energy was proposed by Fertig, Brey, Côté, and MacDonald[8]. These authors also proposed that the ground state away from odd-integer filling factors is a crystal of Skyrmions[9]. In addition, they studied the dynamics of a single Skyrmion bound to a charged impurity[10]. A field-theoretic approach to the low-temperature properties of a multi-Skyrmion system was developed by Green, Kogan, and Tsvelik[11]. The variational wave functions for a single Skyrmion proposed by Fertig *et al.* are eigenstates of $L_z \pm S_z$ (where L_z and S_z are the z components of the orbital and spin angular momentum, respectively), but not of L_z and S_z separately. Skyrmion states that *are* eigenstates of L_z and S_z were found by MacDonald, Fertig, and Brey[12] for a hard-core model Hamiltonian. An alternative variational approach which uses Landau-gauge wave functions (rather than the circular-gauge wave functions used by Fertig *et al.*[8]) has been proposed by Bychkov, Maniv, and Vagner[13]. Numerical studies of Skyrmion excitations at $\nu = 1$ have been carried out by Xie and He[14]. The possible existence of Skyrmions at fractional filling factors (in particular $\nu = \frac{1}{3}$) has been explored by Kamilla, Wu, and Jain[15], and by Ahn and Chang[16].

In this review we give a detailed account of the optical properties of quantum Hall Skyrmions. In particular we address the question of how the optical properties of Skyrmions differ from those of ordinary electrons. Our aim is to provide means for the optical detection of Skyrmions using PL spectroscopy. Brief accounts of parts of this work have been published elsewhere[17,18].

The paper is organized as follows. In Sec. 2 we review the variational description of Skyrmions proposed by Fertig, Brey, Côté, and MacDonald[8]. This approach is very useful for discussing the optical properties of Skyrmions. We also review three key experiments that have given evidence for the existence of Skyrmions at $\nu = 1$. In Sec. 3 we give an overview of the PL experiments that have been carried out on quantum Hall systems, and recall what information these experiments provide. We reproduce the PL spectrum that is experimentally observed near $\nu = 1$ and explain its basic features in terms of a simple model. Sections 4 and 5—which make up the main part of the paper—are concerned with the optical properties of quantum Hall Skyrmions in disordered and pure systems, respectively. The main results of the paper are summarized in Sec. 6.

2. Skyrmions in Quantum Hall Ferromagnets

Consider a 2D electron gas lying in the x-y plane and subjected to a perpendicular magnetic field $\mathbf{B} = B\hat{z}$. The physical properties of the 2D electron gas depend sensitively on the filling factor ν. The filling factor is the ratio between the number of electrons and the orbital degeneracy of a Landau level. Here we consider systems for which the filling factor is an odd integer: $\nu = 1, 3, 5, \ldots$. We focus in particular on the filling factor $\nu = 1$ for which only the lowest Landau level is occupied. In the symmetric gauge with vector potential $\mathbf{A} = \frac{1}{2}B(x, -y, 0)$, the single-particle wave functions for the lowest Landau level have the form[19] (in units where $\ell = \sqrt{\hbar c/eB} = 1$)

$$\phi_m(\mathbf{r}) = (2^{m+1}\pi m!)^{-1/2} r^m e^{-im\phi} e^{-r^2/4}, \tag{1}$$

where $\mathbf{r} = (x, y)$ is the position of the electron in the plane, $r = \sqrt{x^2 + y^2}$ is the magnitude of $\mathbf{r}$, and $\phi = \arctan(y/x)$ is the angle between $\mathbf{r}$ and the x axis. The ground state of the 2D electron gas at filling factor $\nu = 1$ is $|0\rangle = \prod_{m=0}^{\infty} e^{\dagger}_{m\uparrow}|\text{vac}\rangle$, where $|\text{vac}\rangle$ is the empty conduction band, and $e^{\dagger}_{m\uparrow}$ creates a spin-$\uparrow$ electron in the state $\phi_m(\mathbf{r})$. Thus the 2D electron gas at filling factor $\nu = 1$ is a ferromagnet, with all electron spins aligned parallel to the magnetic field[a]. The ground state of the 2D electron gas at higher odd-integer filling factors ($\nu = 3, 5, \ldots$) is also a ferromagnet, in which the lowest ν spin-$\uparrow$ Landau levels and the lowest $(\nu - 1)$ spin-$\downarrow$ Landau levels are completely filled, and all other Landau levels are empty. In the following we study the elementary charged excitations of a 2D electron gas at $\nu = 1$. With a few modifications, the results also apply to the higher odd-integer filling factors $\nu = 3, 5, \ldots$.

2.1. *Elementary charged excitations at* $\nu = 1$

The elementary charged excitations of a 2D electron gas at $\nu = 1$ are the excitations obtained by adding or removing an electron from the state $|0\rangle$. One must keep in mind that at filling factor $\nu = 1$ adding an electron is equivalent to *removing* a flux quantum $\Phi_0 = hc/e$, while removing an electron is equivalent to *adding* a flux quantum[20]. The elementary charged excitations are eigenstates of the Hamiltonian $H = Z + V^{ee}$, where

$$Z = \frac{1}{2}|g_e|\mu_B B \sum_m (e^{\dagger}_{m\downarrow} e_{m\downarrow} + e_{m\uparrow} e^{\dagger}_{m\uparrow}), \tag{2}$$

---

[a] The spins are parallel to the magnetic field—instead of antiparallel, as for free electrons—because the Landé g factor is negative in GaAs.

$$V^{ee} = \frac{1}{2}\sum_{\sigma\sigma'}\sum_{mm'm''m'''} V^{ee}_{mm'm''m'''} e^{\dagger}_{m\sigma} e^{\dagger}_{m'\sigma'} e_{m''\sigma'} e_{m'''\sigma}. \tag{3}$$

Here σ is the spin of an electron ($\sigma = \uparrow$ or $\downarrow$), and $V^{ee}_{mm'm''m'''}$ is a matrix element of the electron-electron interaction $V^{ee}(r) = e^2/\epsilon r$, where ϵ is the background dielectric constant. We have taken the energy of the state $|0\rangle$ as the zero of our energy scale. The nature of the elementary charged excitations is determined by the interplay between the Zeeman energy Z and the electron-electron interaction V^{ee}. It is convenient to introduce the parameter $g = \frac{1}{2}|g_e|\mu_B B/(e^2/\epsilon\ell)$, which is the ratio of the Zeeman energy $\frac{1}{2}|g_e|\mu_B B$ to the typical Coulomb energy $e^2/\epsilon\ell$. For noninteracting electrons ($g = \infty$) the elementary charged excitations are spin-$\downarrow$ electrons ($e^{\dagger}_{m\downarrow}|0\rangle$) and spin-$\uparrow$ holes ($e_{m\uparrow}|0\rangle$). For large but finite g the electron-electron interaction can be treated using perturbation theory. Because V^{ee} contains no terms that flip the spin of an electron, the elementary charged excitations at large g still have spin $\frac{1}{2}$. However, as g is lowered the nature of the elementary charged excitations changes dramatically—they become Skyrmions.

Skyrmions are twists in the spin density of the 2D electron gas. Figure 1 shows a slice of the spin profile of a Skyrmion along the x axis. The full spin profile is obtained by rotating the slice around a vertical axis through $x = 0$ (the z axis). Figures 1(a) and 1(b) show the spin profile of a negatively and a positively charged Skyrmion, respectively. The spin points down at the center of the Skyrmion ($x = 0$). As one moves radially outward the spin rotates smoothly until it points up at the edge of the Skyrmion ($x = \pm\lambda$). To understand the connection between the sense of the spin twist and the charge of the Skyrmion we trace the spin along a circular path lying in a plane perpendicular to the paper (the x-y plane) that encloses the center of the Skyrmion. For the negatively charged Skyrmion shown in Fig. 1(a) the spin precesses as if a magnetic flux $-\Phi_0$ had been inserted at the origin. Since at $\nu = 1$ removing a flux quantum is equivalent to adding an electron, the spin twist in Fig. 1(a) has charge $-e$. For the positively charged Skyrmion shown in Fig. 1(b) the spin precesses in the opposite sense yielding an excitation with charge $+e$.

2.2. *Variational approach to Skyrmions*

Because Skyrmions have a spin much larger than $\frac{1}{2}$ one cannot calculate their energy by starting from the noninteracting case and treating V^{ee} using perturbation theory. A similar situation arises in superconductivity, where the energy of the superconducting state cannot be obtained from the normal state by treating the pairing interaction between the electrons using perturbation theory. The BCS treatment of the superconducting state provides a clue for the description of Skyrmions. The variational states proposed by Fertig, Brey, Côté, and MacDonald[8] are

$$|\psi_-\rangle = \prod_{m=0}^{\infty}(u_m e^{\dagger}_{m\downarrow} e_{m+1\uparrow} + v_m) e_{0\uparrow}|0\rangle, \tag{4}$$

$$|\psi_+\rangle = \prod_{m=0}^{\infty}(-u_m e^{\dagger}_{m+1\downarrow} e_{m\uparrow} + v_m) e^{\dagger}_{0\downarrow}|0\rangle. \tag{5}$$

The state $|\psi_-\rangle$ ($|\psi_+\rangle$) describes a positively (negatively) charged Skyrmion localized at the origin of the x-y plane[b]. The state $|\psi_-\rangle$ ($|\psi_+\rangle$) is analogous to the BCS state[22], except that the pairing now occurs between a spin-↓ electron (spin-↑ hole) in the mth angular momentum state and a spin-↑ hole (spin-↓ electron) in the $(m+1)$th angular momentum state of the lowest Landau level.

The energy of the Skyrmion is obtained by minimizing the expectation value of H in the state $|\psi_\pm\rangle$, subject to the constraint $|u_m|^2 + |v_m|^2 = 1$. Figure 2 shows the energy and spin of a negatively charged Skyrmion as a function of the parameter g. The energy of a spin-$\frac{1}{2}$ quasielectron is also shown for comparison. A positively charged Skyrmion has the same energy (up to a g-independent constant) and spin as a negatively charged Skyrmion[8]. The size of the stable spin twist is determined by a competition between the Zeeman energy, which opposes spin flips (and hence tries to minimize λ), and the exchange interaction, which favors a gradual spin reversal (and therefore tries to maximize λ). At large g the energy cost of flipping spins is prohibitive and the lowest energy excitation is a spin-$\frac{1}{2}$ quasiparticle. As g is lowered the size of the Skyrmion increases and its energy falls below that of a spin-$\frac{1}{2}$ quasiparticle. Near $g = 0$ the Skyrmion becomes a macroscopic object whose size is determined by the sample boundary.

2.3. *Experimental evidence for Skyrmions*

The first experimental evidence for large-spin charged excitations near $\nu = 1$ was obtained by Barrett, Dabbagh, Pfeiffer, West, and Tycko[4] using an optically pumped NMR technique. By measuring the Knight shift of ^{71}Ga nuclei embedded in a quantum well these authors were able to determine the degree of spin polarization of the 2D electron gas as a function of the filling factor ν. If the charged excitations were spin-$\frac{1}{2}$ quasiparticles one would expect the spin polarization to remain constant for $\nu < 1$, and decline gradually for $\nu > 1$. Instead, Barrett and coworkers observed a rapid decrease of the spin polarization on *both* sides of $\nu = 1$. This is consistent with positively and negatively charged excitations of large and equal spin—i.e. Skyrmions.

Further evidence supporting the existence of Skyrmions at $\nu = 1$ was provided by Schmeller, Eisenstein, Pfeiffer, and West[5]. They performed activated magnetotransport measurements of the energy gap Δ for creating a *pair* of quasiparticles at $\nu = 1$. The energy gap is found from the temperature dependence of the longitudinal resistance using $R_{xx} = R_0 \exp(-\Delta/2k_BT)$. The spin s of the quasiparticle pair is obtained by measuring the change in Δ produced by tilting the total magnetic field B_{tot} away from the normal to the 2D plane (while keeping the perpendicular field $B_\perp$ constant). The energy gap is given by

$$\Delta = \Delta_0(B_\perp) + s|g_e|\mu_B B_{\text{tot}}. \tag{6}$$

The first term, $\Delta_0(B_\perp)$, is the contribution to the energy gap from V^{ee}. For an infinitely thin 2D electron gas this term only depends on the perpendicular field controlling the orbital motion. The second term is the Zeeman energy of the quasiparticle pair. According to Eq. (6) the slope $\partial\Delta/\partial B_{\rm tot}$ at constant $B_\perp$ is just $s|g_e|\mu_B$. Schmeller and company measured the variation of Δ with $B_{\rm tot}$ in GaAs quantum wells at several odd-integer filling factors. At $\nu = 3$ and $\nu = 5$ they observed slopes with $s = 1$, as expected for a pair of spin-$\frac{1}{2}$ quasiparticles. However, at $\nu = 1$ they observed a much larger slope with $s \approx 7$. This implies that the quasiparticles at $\nu = 1$ (but not those at $\nu = 3$ and $\nu = 5$) are Skyrmions with a spin of approximately 3.5.

---

[b] The subscript ± on $|\psi_\pm\rangle$ denotes the sign of the topological charge $Q = \pm 1$. The electric charge is given by $-Qe$.

Evidence for Skyrmions at $\nu = 1$ was also obtained by Aifer, Goldberg and Broido[6] using interband optical transmission spectroscopy. Their experiment consisted of a measurement of the absorption coefficients for right and left circularly polarized (RCP and LCP) light as a function of filling factor between $\nu = 0.6$ and $\nu = 1.4$. In a simple model[6] the absorption coefficient for RCP (LCP) light is proportional to the number of available (i.e. unoccupied) states $N_{A_\downarrow}$ ($N_{A_\uparrow}$) in the spin-$\downarrow$ (spin-$\uparrow$) lowest Landau level. The number of available states, N_{A_σ} ($\sigma = \downarrow$ or $\uparrow$), is related to the number of occupied states (N_σ) by $N_{A_\sigma} = N_B - N_\sigma$, where N_B is the Landau level degeneracy. The spin polarization per electron is $S_z = (N_\downarrow - N_\uparrow)/N$, where $N = N_\downarrow + N_\uparrow$ is the total number of electrons. The difference between the RCP and LCP absorption intensities thus provides a direct measurement of the degree of spin polarization of the electron gas. Using this technique, Aifer and coworkers found a rapid decay of the spin polarization on *both* sides of $\nu = 1$, which is inconsistent with quasiparticles of spin $\frac{1}{2}$. From the rate of decay of the spin polarization they deduced values of 2.5 and 3.7 for the Skyrmion spin in their samples.

3. PL Spectroscopy of Quantum Hall Systems

Spectroscopic methods based on the radiative recombination of 2D electrons with photoexcited holes have developed into a powerful tool for studying the quantum Hall effect. Optical measurements can give information about fundamental aspects of quantum Hall systems. For example, photoluminescence (PL) and photoluminescence excitation (PLE) measurements yield transition energies, polarization studies are sensitive to the electron spin, and ultrafast pump-and-probe experiments monitor carrier relaxation processes on a sub-picosecond timescale. In this work we consider the PL spectroscopy of quantum Hall systems near $\nu = 1$.

3.1. *Intrinsic and extrinsic PL*

PL studies of quantum Hall systems can be divided into two types according to the experimental setup employed. *Intrinsic* PL experiments study the recombination of 2D electrons with photoexcited holes in standard GaAs/Ga$_{1-x}$Al$_x$As heterojunctions and quantum wells[23,24,25,26]. Figure 3 shows the band diagram of a one-side modulation-doped GaAs/Ga$_{1-x}$Al$_x$As quantum well. The structure consists of a GaAs layer sandwiched between two $\mathrm{Ga}_{1-x}\mathrm{Al}_x\mathrm{As}$ barriers. Only the left $\mathrm{Ga}_{1-x}\mathrm{Al}_x\mathrm{As}$ barrier is doped, leading to an asymmetric band profile. The energy spectrum in the absence of a magnetic field consists of a series of conduction and valence subbands[27]. Only the lowest conduction subband (E_0) and the highest valence subband (HH_0) are shown in Fig. 3, along with the corresponding z wave functions. The electrons are confined near the interface between the GaAs layer and the left $\mathrm{Ga}_{1-x}\mathrm{Al}_x\mathrm{As}$ barrier, while the holes are confined on the opposite side of the well, near the interface between the GaAs layer and the right $\mathrm{Ga}_{1-x}\mathrm{Al}_x\mathrm{As}$ barrier. The dotted lines indicate the average positions of the electrons and holes along z. For simplicity we consider a model in which the electrons and holes are confined to infinitely thin planes separated by a distance d. This amounts to approximating the z wave functions by δ functions. The effect of the finite extent of the z wave functions on the PL spectrum is discussed in Sec. 4.7.

Extrinsic PL experiments utilise specialized structures, in which a δ-doped layer of acceptors is grown into the GaAs at a certain distance from the $\mathrm{Ga}_{1-x}\mathrm{Al}_x\mathrm{As}$–GaAs interface[28,29,30]. The recombination studied in extrinsic PL is between a 2D electron and a hole bound to an acceptor in the δ-doped layer. Extrinsic PL is quite different from intrinsic PL because the acceptor is charge *neutral* in the initial state. The type of PL considered in this work is intrinsic PL.

An intrinsic PL experiment consists of three stages. In the first stage electrons are promoted from the GaAs valence band into the GaAs conduction band by a pump laser tuned below the $\mathrm{Ga}_{1-x}\mathrm{Al}_x\mathrm{As}$ band gap. Pump intensities are kept low ($< 10^{-4}$ Wcm^{-2}) to prevent heating of the electron gas. In the second stage the photoexcited carriers relax to the lowest energy state within their respective energy bands. The intraband relaxation takes place on a timescale (picoseconds) which is short compared to the radiative recombination time (nanoseconds). In the third stage the photoexcited holes recombine with either photoexcited electrons or 2D electrons. Recording the number of emitted photons of frequency ω and polarization α ($\alpha = +1$ for RCP and $\alpha = -1$ for LCP) yields the (polarization-resolved) PL spectrum $P_\alpha(\omega)$.

3.2. *PL spectrum*

According to the Fermi Golden Rule, the PL spectrum is given by

$$P_\alpha(\omega) = 2\pi \sum_{i,f} n_i |\langle f|L_\alpha|i\rangle|^2 \delta(\omega - E_i + E_f). \tag{7}$$

Here $|i\rangle$ ($|f\rangle$) is the initial (final) state before (after) recombination, n_i is the occupation of initial states, and L_α is the luminescence operator (given further below). The energy ω of the emitted photon is equal to the difference between the energy of the initial state (E_i) and the energy of the final state (E_f). Assuming complete relaxation of the photoexcited carriers prior to recombination, the occupation of initial states is $n_i = \frac{1}{Z} e^{-E_i/k_B T}$, where $Z = \sum_i e^{-E_i/k_B T}$ is the partition function at temperature T. PL studies of quantum Hall systems are done at temperatures as low as $T = 0.1$ K (corresponding to an energy of about 0.01 meV). At these temperatures only the initial state with the lowest energy, $|i_0\rangle$, has significant occupation. Setting $n_i = \delta_{i,i_0}$ in Eq. (7),

$$P_\alpha(\omega) = 2\pi \sum_f |\langle f|L_\alpha|i_0\rangle|^2 \delta(\omega - E_{i_0} + E_f), \tag{8}$$

where E_{i_0} is the energy of the state $|i_0\rangle$. As compared to the ground state $|0\rangle$, the initial state $|i_0\rangle$ has one more negatively charged excitation in the conduction band and a hole in the valence band. Provided the hole does not significantly perturb the electron gas, the negatively charged excitation is precisely the one studied in Sec. 3.1. We may therefore expect to see a signature of Skyrmions in the PL spectrum at $\nu = 1$.

3.3. *PL spectra near* $\nu = 1$

A number of PL studies near $\nu = 1$ have been reported in the literature[23,24,25,26]. Below we summarize the results of two representative studies. Figure 4 shows the results of an experiment by Turberfield *et al.*[23] on a GaAs/Ga$_{0.68}$Al$_{0.32}$As single heterojunction. The figure shows the magnetic-field dependence of the energy of the E_0 luminescence line arising from the recombination of 2D electrons in the lowest conduction subband (E_0) with holes in the GaAs valence band. The inset shows the line shapes at selected magnetic fields near $\nu = 1$. The important features are:

(i) There are two lines on the low-B side of $\nu = 1$, and one line on the high-B side.
(ii) The lower-energy line has an abrupt redshift as the magnetic field is increased past $\nu = 1$.

Polarization-resolved PL studies of GaAs/Ga$_{1-x}$Al$_x$As quantum wells and heterojunctions in the quantum Hall regime have been reported by Goldberg *et al.*[25] The PL spectra in wide quantum wells (with well widths of 400–500 Å) and single heterojunctions have the following features:

(i) There is a RCP line and a LCP line on the low-B side of $\nu = 1$, and only a LCP line on the high-B side.
(ii) The LCP line has an abrupt redshift as the magnetic field is increased past $\nu = 1$.

The important features of the PL spectrum near $\nu = 1$ can be explained using a simple model[31,32] in which the electrons occupy the lowest Landau level of the E_0 conduction subband, and the holes occupy the highest Landau level of the HH_0 valence subband (see Fig. 3). The electrons have spin ↑ or ↓, and the holes have $m_j = \pm\frac{3}{2}$. The lowest-energy transition in LCP is from the spin-↑ electron state to the $m_j = +\frac{3}{2}$ hole state, and the lowest-energy transition in RCP is from the spin-↓ electron state to the $m_j = -\frac{3}{2}$ hole state.

In Fig. 5 we compare a PL experiment at $\nu = 1$ with a PL experiment at the filling factor just below $\nu = 1$ where one spin-$\uparrow$ electron is missing from the lowest Landau level [Fig. 5(a)]. We denote this filling factor by $\nu = 1^-$. At $\nu = 1$ the state before recombination has one extra spin-$\downarrow$ electron and a valence hole [Fig. 5(b)]. The photoexcited electron must have spin $\downarrow$ because the spin-$\uparrow$ Landau level is completely filled. At $\nu = 1^-$ the state before recombination has a filled spin-$\uparrow$ level and a valence hole. The photoexcited electron has filled up the hole in the spin-$\uparrow$ Landau level that was present in the ground state at $\nu = 1^-$.

In the LCP transition a spin-$\uparrow$ electron recombines with a $m_j = +\frac{3}{2}$ hole. This transition can take place both at $\nu = 1$ and at $\nu = 1^-$ [Fig. 5(c)]. We thus expect to see a LCP line on both sides of $\nu = 1$. In the RCP transition a spin-$\downarrow$ electron recombines with a $m_j = -\frac{3}{2}$ hole. This transition *can* take place at $\nu = 1$, but *not* at $\nu = 1^-$, where no spin-$\downarrow$ electrons are available in the initial state [Fig. 5(d)]. We thus expect to see a RCP line on the low-B side of $\nu = 1$, but not on the high-B side.

To explain the redshift of the LCP line we compare the states before and after LCP recombination at $\nu = 1$ and $\nu = 1^-$ [Figs. 5(b) and (c)]. The spin-$\downarrow$ electron and the valence hole in the initial state at $\nu = 1$ will bind to form an interband exciton. This means the initial state at $\nu = 1$ has a lower energy than the initial state at $\nu = 1^-$, which has an unbound valence hole. The energy difference is $\Delta E_i = -B_X$, where B_X is the binding energy of the interband exciton[32]. Similarly, the spin-$\downarrow$ electron and the spin-$\uparrow$ hole in the final state at $\nu = 1$ will bind to form a spin wave. Hence the final state at $\nu = 1$ has a lower energy than the final state at $\nu = 1^-$, which has an unbound spin-$\uparrow$ hole. The energy difference between the final states is $\Delta E_f = -B_{SW}$, where B_{SW} is the binding energy of the spin wave[32]. The shift of the LCP luminescence line is given by $\Delta\omega = \Delta E_i - \Delta E_f = B_{SW} - B_X$. Because the spin-$\downarrow$ electron and the valence hole are spatially separated along z, while the spin-$\downarrow$ electron and the spin-$\uparrow$ hole are both in the same plane, the spin wave has a larger binding energy than the interband exciton. Hence the LCP line shifts to *lower* energies (redshift) as the magnetic field is increased past $\nu = 1$.

4. Optics with Skyrmions in Disordered Systems

The simple model discussed in Sec. 3.3 is based on a quasiparticle picture of the charged excitations at $\nu = 1$. What if the charged excitations were Skyrmions, instead of spin-$\frac{1}{2}$ quasiparticles? In what way does the recombination spectrum of Skyrmion differ from that of a spin-$\frac{1}{2}$ quasielectron? These are the questions this section aims to address.

Besides being of interest for the PL spectrum at $\nu = 1$, these questions are also of broader relevance to the optical properties of quantum Hall systems at other filling factors. The $\nu = 1$ state serves as a prototype for spin-polarized states at higher odd-integer filling factors ($\nu = 3, 5, \ldots$), and, via the composite-fermion picture[33], also for spin-polarized states at fractional filling factors ($\nu = \frac{1}{3}, \frac{2}{5}, \ldots$). Indeed, it has been suggested[15] that the elementary charged excitations at $\nu = \frac{1}{3}, \frac{2}{5}, \ldots$

can be regarded as Skyrmions of composite fermions. An understanding of the recombination spectrum at $\nu = 1$ could therefore provide important clues about the recombination spectrum of spin-polarized states at other filling factors.

We start our investigation of the optical properties of Skyrmions with a study of disordered systems. The localization of the photoexcited hole by the disorder potential considerably simplifies the mathematical treatment of the initial state. The optical properties of Skyrmions in pure systems are discussed in Sec. 5.

4.1. *Sources of disorder*

Sources of disorder in a modulation-doped quantum well of the type shown in Fig. 3 include:

- Ionized impurities in the doped layer.
- Residual impurities in the undoped layers.
- Roughness of the interface between the GaAs and $\mathrm{Ga}_{1-x}\mathrm{Al}_x\mathrm{As}$ layers.
- Fluctuations in the alloy composition of the $\mathrm{Ga}_{1-x}\mathrm{Al}_x\mathrm{As}$ layers.

To model the disorder we introduce disorder potentials $V^e(\mathbf{r})$ and $V^h(\mathbf{r})$ acting on the electrons and holes, respectively. The dominant contribution to $V^e(\mathbf{r})$ comes from ionized impurities in the doped layer. To achieve a higher electron mobility an undoped spacer layer is grown between the doped layer and the GaAs well (see Fig. 3). The ability to spatially separate the electrons from the donor impurities accounts for the extremely high mobilities achieved in modulation-doped heterostructures when compared to bulk semiconductors. The larger separation between the doped layer and the holes reduces the contribution of this type of disorder to $V^h(\mathbf{r})$.

Disorder due to interface roughness is expected to dominate $V^h(\mathbf{r})$. The holes are confined near the so-called "inverted" interface (i.e. GaAs grown on top of $\mathrm{Ga}_{1-x}\mathrm{Al}_x\mathrm{As}$) which is known[34] to have a higher degree of disorder than the "normal" interface ($\mathrm{Ga}_{1-x}\mathrm{Al}_x\mathrm{As}$ on top of GaAs). It was, in fact, the difficulty of growing a smooth inverted interface that prompted the introduction of the one-side modulation-doped quantum well[35]. Doping only on the side of the normal interface pulls the electrons away from the inverted interface[36], thus significantly reducing the contribution of this type of disorder to $V^e(\mathbf{r})$.

In the following we neglect $V^e(\mathbf{r})$ compared to $V^h(\mathbf{r})$. This is reasonable given the very high mobility of the samples used in recent experiments[23,25]. Note that $V^h(\mathbf{r})$ does not affect the mobility because no holes are present prior to illumination.

4.2. *Initial state in a disordered system*

Consider the optical recombination of a Skyrmion with a hole localized near a minimum in $V^h(\mathbf{r})$. We choose the location of the minimum as the origin of our coordinate system. Provided the disorder potential varies slowly on the scale of ℓ, the hole is in the $m = 0$ state. The Skyrmion also becomes localized near the origin due to the Coulomb attraction between the Skyrmion and the hole. Assuming complete energy relaxation prior to recombination, the initial state is given by

$$|i_0\rangle = \prod_{m=0}^{\infty}(-u_m e^{\dagger}_{m+1\downarrow} + v_m e^{\dagger}_{m\uparrow})e^{\dagger}_{0\downarrow}h^{\dagger}_{0m_j}|\mathrm{vac}\rangle. \tag{9}$$

The parameters u_m and v_m are determined by minimizing the expectation value of $H = \varepsilon^h_{0m_j} + Z + V^{ee} + V^{eh}$ in the state $|i_0\rangle$, subject to the constraint $|u_m|^2 + |v_m|^2 = 1$. Here

$$\varepsilon^h_{0m_j} = E_g + \frac{eB}{2\mu c} + m_j g_h \mu_B B \tag{10}$$

is the energy of the hole[c], where E_g is the bandgap at zero magnetic field, $\mu = m_e m_h/(m_e + m_h)$ is the reduced mass, and g_h is the Landé g-factor for the hole. Z and V^{ee} are given by Eqs. (2) and (3), respectively, and

$$V^{eh} = \sum_{\sigma, m_j}\sum_{mm'm''m'''} V^{eh}_{mm'm''m'''} e^{\dagger}_{m\sigma} h^{\dagger}_{m'm_j} h_{m''m_j} e_{m'''\sigma} \tag{11}$$

is the electron-hole interaction. Here $V^{eh}_{mm'm''m'''}$ is a matrix element of $V^{eh}(\mathbf{r}) = e^2/\epsilon|\mathbf{r} + \hat{z}d|$, where d is the separation between the electron and hole planes along z (see Fig. 3).

To evaluate the expectation value we use the relations

$$\begin{aligned}
\langle i_0|e^{\dagger}_{m\downarrow}e_{m\downarrow}|i_0\rangle &= |u_{m-1}|^2, & (12)\\
\langle i_0|e^{\dagger}_{m\uparrow}e_{m\uparrow}|i_0\rangle &= |v_m|^2, & (13)\\
\langle i_0|e^{\dagger}_{m+1\downarrow}e_{m\uparrow}|i_0\rangle &= -u^*_m v_m. & (14)
\end{aligned}$$

The first (second) relation gives the probability of finding an electron with spin ↓ (↑) in the mth angular momentum state. We define $u_{-1} \equiv -1$ and $v_{-1} \equiv 0$ to account for the definite occupation of the $m = 0$ state by a spin-↓ electron. The third relation expresses the pairing correlation between a spin-↓ electron in the $(m+1)$th angular momentum state and a spin-↑ electron in the mth angular momentum state. With the aid of these relations we find

$$\langle i_0|H|i_0\rangle = \varepsilon^h_{0m_j} + U^Z + U^H - U^{ex} - U^{sk} - U^{eh}, \tag{15}$$

where

$$\begin{aligned}
U^Z &= \frac{1}{2}|g_e|\mu_B B \sum_{m=0}^{\infty}(|u_{m-1}|^2 - |v_m|^2 + 1), & (16)\\
U^H &= \frac{1}{2}\sum_{m,m'=0}^{\infty} V^{ee}_{mm'm'm}(|u_{m-1}|^2 + |v_m|^2 - 1)(|u_{m'-1}|^2 + |v_{m'}|^2 - 1), & (17)
\end{aligned}$$

---

[c] Recall that we have chosen the energy of the state $|0\rangle$ as the zero of our energy scale.

$$U^{ex} = \frac{1}{2}\sum_{m,m'=0}^{\infty} V^{ee}_{mm'mm'}(|u_{m-1}|^2|u_{m'-1}|^2 + |v_m|^2|v_{m'}|^2 - 1), \tag{18}$$

$$U^{sk} = \sum_{m,m'=0}^{\infty} V^{ee}_{mm'm-1m'+1}u^*_{m-1}v_{m-1}u_{m'}v^*_{m'}, \tag{19}$$

$$U^{eh} = \sum_{m=0}^{\infty} V^{eh}_{m00m}(|u_{m-1}|^2 + |v_m|^2 - 1). \tag{20}$$

The expectation value of H is the sum of six terms. The first term is the energy of the hole. The second term (U^Z) is the Zeeman energy of the Skyrmion. Since $u_m \to 0$ and $v_m \to 1$ when $m \to \infty$ the sum over m converges. The third term (U^H) has contributions from the direct Coulomb interaction among the electrons (Hartree energy), the Coulomb interaction between the electrons and the positive background, and the Coulomb energy of the positive background itself. The fourth term (U^{ex}) is exchange interaction between electrons of parallel spin. The factor of -1 inside the parentheses comes from subtracting the exchange energy of the state $|0\rangle$. The fifth term (U^{sk}) is the correlation energy which arises from the pairing of a spin-$\downarrow$ electron in the $(m+1)$th angular momentum state with a spin-$\uparrow$ electron in the mth angular momentum state. Finally, the sixth term (U^{eh}) is the Coulomb interaction between the electrons and the hole.

The results of a numerical minimization of $\langle i_0|H|i_0\rangle$ are shown in Fig. 6. Figure 6(a) shows the difference between the minimized energy of the state $|i_0\rangle$ (consisting of a Skyrmion and a hole) and the energy of the state $e^\dagger_{0\downarrow}h^\dagger_{0m_j}|0\rangle$ (consisting of an spin-$\downarrow$ electron and a hole against a $\nu = 1$ background). Figure 6(b) shows the corresponding difference in spin between the two states. The energy and spin of the Skyrmion are determined by three competing effects. As in Fig. 2 the Skyrmion shrinks with increasing Zeeman coupling. The difference between the state $|i_0\rangle$ and the state $|\psi_+\rangle$ is the presence of the photoexcited hole. The electron-hole interaction favors a charge distribution for the electrons that is strongly peaked in the vicinity of the hole and therefore Skyrmions of small size. Bringing the hole closer to the electron plane increases the strength of the electron-hole interaction, thereby reducing the Skyrmion size. Upon decreasing g at a fixed value of d there is a threshold to Skyrmion formation. When the hole is far away from the electron plane ($d = \infty$) the threshold value of g is approximately 0.025. Reducing d lowers the value of g below which Skyrmions form. When the hole comes too close to the electron plane ($d < \ell$) there is no Skyrmion formation at any value of g. Thus we may expect to see an optical signature of Skyrmions in wide ($d > \ell$) quantum wells, but not in narrow ($d < \ell$) wells.

4.3. *Moments of the PL spectrum*

We treat the optical recombination in the electric-dipole approximation. The luminescence operators for RCP and LCP transitions are given by

$$L_+ = \mu_+ \sum_m e_{m\downarrow} h_{m,-3/2}, \tag{21}$$

$$L_- = \mu_- \sum_m e_{m\uparrow} h_{m,3/2}, \tag{22}$$

respectively, where $\mu_\pm$ is the product of the interband dipole matrix element and the overlap between the electron and hole z wave functions. There is an important difference between the optical recombination of a spin-$\frac{1}{2}$ quasielectron and the optical recombination of a Skyrmion. While recombination of a spin-$\frac{1}{2}$ quasielectron leaves either no spin flips (in the case of RCP) or one spin flip (in the case of LCP) in the final state, recombination of a Skyrmion leaves a large number of spin flips in the final state. For a Skyrmion with spin S_z, the number of spin flips left is $|S_z + \frac{1}{2}|$ in the case of RCP, and $|S_z - \frac{1}{2}|$ in the case of LCP.

The PL spectrum is given by Eq. (8). The detailed line shape is difficult to calculate owing to the complicated nature of the final states containing multiple spin flips. However, the existing PL studies discussed in Sec. 3.3 suggest that the quantity of primary interest is the luminescence energy

$$\langle \omega_\alpha \rangle = \int d\omega\, \omega P_\alpha(\omega). \tag{23}$$

The usefulness of moments of the PL spectrum was demonstrated by Apalkov and Rashba[38] in the context of the fractional quantum Hall effect. The luminescence energy (and other moments of the spectrum) can be obtained directly from the initial state $|i_0\rangle$. Integrating Eq. (8) with respect to ω we obtain

$$\langle \omega_\alpha \rangle = 2\pi \sum_f (E_{i_0} - E_f) |\langle f | L_\alpha | i_0 \rangle|^2. \tag{24}$$

If $|i_0\rangle$ and $|f\rangle$ are eigenstates of H (i.e. $H|i_0\rangle = E_{i_0}|i_0\rangle$ and $H|f\rangle = E_f|f\rangle$) this can be written as

$$\langle \omega_\alpha \rangle = 2\pi \sum_f \langle i_0 | L_\alpha^\dagger | f \rangle \langle f | [L_\alpha, H] | i_0 \rangle, \tag{25}$$

where $[L_\alpha, H] = L_\alpha H - H L_\alpha$. We now sum over all final states within the lowest Landau level. This yields the projection operator $P = \sum_f |f\rangle\langle f|$ onto the lowest Landau level. Since L_α, H, and $|i_0\rangle$ are already in the lowest Landau level, the projection operator acts as the unit operator. Hence

$$\langle \omega_\alpha \rangle = 2\pi \langle i_0 | L_\alpha^\dagger [L_\alpha, H] | i_0 \rangle. \tag{26}$$

Expressions for the other moments can be derived in a similar way. The nth-order moment $\langle \omega_\alpha^n \rangle = \int d\omega\, \omega^n P_\alpha(\omega)$ is given by

$$\langle \omega_\alpha^n \rangle = 2\pi \langle i_0 | L_\alpha^\dagger [L_\alpha, H]_n | i_0 \rangle, \tag{27}$$

where $[L_\alpha, H]_n$ is defined by $[L_\alpha, H]_n = [[L_\alpha, H]_{n-1}, H]$ and $[L_\alpha, H]_0 = L_\alpha$. It is convenient to redefine $\langle \omega_\alpha^n \rangle = \langle \omega_\alpha^n \rangle / \langle \omega_\alpha^0 \rangle$, where $\langle \omega_\alpha^0 \rangle$ is the integrated intensity.

4.4. *PL energies*

To calculate the energies of the RCP and LCP lines we use Eq. (27) with $n = 0, 1$ and the initial state given by Eq. (9). Working out the commutator and applying Eqs. (12)–(14), we find

$$\begin{aligned} \langle \omega_+ \rangle &= \varepsilon^h_{0,-3/2} + \varepsilon^e_{0\downarrow} - U^{eh}_{0\downarrow}, && (28) \\ \langle \omega_- \rangle &= \varepsilon^h_{0,3/2} + E^e_{0\uparrow} - U^{eh}_{0\uparrow}, && (29) \end{aligned}$$

where

$$\begin{aligned} U^{eh}_{0\uparrow} &= V^{eh}_{0000} + \sum_{m=2}^{\infty} V^{eh}_{m00m} |u_{m-1}|^2 + \sum_{m=1}^{\infty} V^{eh}_{m00m} |v_m|^2, && (30) \\ U^{eh}_{0\downarrow} &= \sum_{m=1}^{\infty} V^{eh}_{m00m} |u_{m-1}|^2 + \sum_{m=0}^{\infty} V^{eh}_{m00m} |v_m|^2, && (31) \end{aligned}$$

and

$$E^e_{0\uparrow} = \frac{\varepsilon^e_{1\downarrow} + \varepsilon^e_{0\uparrow}}{2} - \sqrt{\left(\frac{\varepsilon^e_{1\downarrow} - \varepsilon^e_{0\uparrow}}{2} \right)^2 + |U^{sk}_0|^2}, \qquad (32)$$

with

$$\begin{aligned} \varepsilon^e_{m\uparrow} &= -\frac{1}{2} |g_e| \mu_B B + U^H_m - U^{ex}_{m\uparrow} - V^{eh}_{m00m}, && (33) \\ \varepsilon^e_{m\downarrow} &= \frac{1}{2} |g_e| \mu_B B + U^H_m - U^{ex}_{m\downarrow} - V^{eh}_{m00m}, && (34) \end{aligned}$$

and

$$\begin{aligned} U^H_m &= \sum_{m'=0}^{\infty} V^{ee}_{mm'm'm} (|u_{m'-1}|^2 + |v_{m'}|^2 - 1), && (35) \\ U^{ex}_{m\uparrow} &= \sum_{m'=0}^{\infty} V^{ee}_{mm'mm'} |v_{m'}|^2, && (36) \\ U^{ex}_{m\downarrow} &= \sum_{m'=0}^{\infty} V^{ee}_{mm'mm'} |u_{m'-1}|^2, && (37) \\ U^{sk}_m &= \sum_{m'=0}^{\infty} V^{ee}_{mm'+1\,m+1\,m'} u^*_{m'} v_{m'}. && (38) \end{aligned}$$

The RCP luminescence energy given by Eq. (28) is the sum of three terms. The first term ($\varepsilon^h_{0,-3/2}$) is the energy of the hole. The second term ($\varepsilon^e_{0\downarrow}$) is the energy of the spin-↓ electron at the center of the Skyrmion. The third term ($U^{eh}_{0\downarrow}$) is the Coulomb interaction between the remaining electrons (i.e. all those *except* the spin-↓

electron at the center) and the valence hole. The LCP luminescence energy given by Eq. (29) also has three terms, of which only the second term ($E^e_{0\uparrow}$) needs further explanation. This term represents the energy of the spin-$\uparrow$ electron at the the center of the Skyrmion. Removing a spin-$\uparrow$ electron from the $m = 0$ state breaks the pair bond with the spin-$\downarrow$ electron in the $m = 1$ state. Hence $E^e_{0\uparrow}$ involves not only $\varepsilon^e_{0\uparrow}$, but also $\varepsilon^e_{1\downarrow}$ and the pair interaction U^{sk}_0.

In Fig. 7 we show the mean luminescence energy

$$\langle\omega\rangle = \frac{\langle\omega_+\rangle + \langle\omega_-\rangle}{2} \tag{39}$$

as a function of g and d. Starting from $g = 0$, the mean luminescence energy increases monotonically until g reaches a threshold g_c. Above the threshold $\langle\omega\rangle$ does not vary with g. The threshold is $g_c = 0.025$ when $d = \infty$ and becomes smaller as the hole is brought closer to the electron plane. By setting $u_m = 0$ and $v_m = 1$ in Eqs. (28)–(38) (but keeping $u_{-1} = -1$) we can show that for a spin-$\frac{1}{2}$ quasielectron $\langle\omega\rangle$ does *not* depend on g. Hence a variation of $\langle\omega\rangle$ with g signals the presence of Skyrmions in the initial state.

4.5. *Redshift*

We now consider the PL spectrum at filling factor $\nu = 1^-$. In the context of the present model—which includes disorder for the hole—the initial state at $\nu = 1^-$ is given by $|i_0\rangle = h^\dagger_{0m_j}|0\rangle$. The energy of this state is

$$E_{i_0} = \varepsilon^h_{0m_j} - \sum_{m=0}^{\infty} V^{eh}_{m00m}. \tag{40}$$

Since there are no spin-$\downarrow$ electrons in the initial state the RCP line is missing from the PL spectrum. The final state after LCP recombination is $|f\rangle = e_{0\uparrow}|0\rangle$ with energy

$$E_f = \frac{1}{2}|g_e|\mu_B B + \sum_{m=0}^{\infty} V^{ee}_{m0m0}. \tag{41}$$

Thus the PL spectrum at $\nu = 1^-$ consists of a single LCP line at

$$\omega_- = \varepsilon^h_{0,3/2} - \frac{1}{2}|g_e|\mu_B B - \sum_{m=0}^{\infty} V^{ee}_{m0m0} - \sum_{m=0}^{\infty} V^{eh}_{m00m}. \tag{42}$$

The redshift of the LCP line is given by the difference between Eq. (29) and Eq. (42). For a spin-$\frac{1}{2}$ quasielectron the redshift *does not* depend on g. Setting $u_m = 0$ and $v_m = 1$ we find

$$\Delta\omega_- = V^{ee}_{0000} - V^{eh}_{0000}. \tag{43}$$

For a Skyrmion the redshift *does* depend on g. Hence a measurement of the g dependence of the redshift provides a way to distinguish between the optical recombination of a Skyrmion and the optical recombination of a spin-$\frac{1}{2}$ quasielectron.

In practice g may be varied by tilting the magnetic field away from the normal to the 2D plane or by applying hydrostatic pressure. The tilted-field method was discussed earlier in Sec. 2.3. While the spin couples to the total field ($B_{\rm tot}$), the orbital motion is controlled by the perpendicular field ($B_\perp$). Hence $g = g_\perp / \cos\theta$, where $g_\perp = \frac{1}{2}|g_e|\mu_B B_\perp/(e^2/\epsilon\ell_\perp)$ (with $\ell_\perp = \sqrt{\hbar c/eB_\perp}$), and θ is the tilting angle. Note that tilting the magnetic field increases g. An alternative way of varying g is by applying hydrostatic pressure[7,39]. The Landé g factor in GaAs ($g_e = -0.44$) differs from the g factor for free electrons ($g_e = 2.0$) due to the mixing between the conduction band and the spin-orbit split valence band. Applying hydrostatic pressure increases the bandgap, thereby reducing the amount of mixing between the two bands. As a result the g factor becomes more free-electron like when pressure is applied. The variation of g_e with applied pressure has been calculated by Holmes *et al.*[39] using $\mathbf{k}\cdot\mathbf{p}$ perturbation theory. In the pressure range from 0 to 10 kbar they find $g_e = -0.43 + 0.02p$, where p is the pressure (in kbar). Note that $|g_e|$ *decreases* upon applying pressure.

In Fig. 8 we show the calculated variation of the redshift with tilting angle (θ) and applied pressure (p), for a GaAs/Ga$_{1-x}$Al$_x$As quantum well with $n_s = 10^{11}$ cm^{-2} and a separation of 400 Å between the electron and hole planes. Upon tilting the field by 60° the red shift increases by 0.6 meV, while raising the pressure from 1 to 10 kbar reduces the red shift by 0.4 meV. In both cases the change of the redshift is well within the experimental resolution (typically 0.1 meV).

4.6. *Finite-size effect*

Thus far we have considered a model in which the electrons and the hole are confined to infinitely thin planes separated by a distance d. In reality the electron and hole wave functions have a finite extent along z (Fig. 3). We now discuss the effect of the finite extent of the z wave functions on the PL spectrum for two particular device designs used in recent experiments: an asymmetric quantum well, and a single heterojunction.

We first consider the tilted-field experiment for an asymmetric quantum well. The parallel component of the magnetic field ($B_\parallel$) causes a diamagnetic shift of the electron and hole subband energies (E_0 and HH_0). This leads to an additional θ dependence of the PL energy, which does not occur in the strictly 2D system. For a weak parallel field the diamagnetic shift may be calculated using perturbation theory[40]. The additional θ dependence of the PL energy is then given by

$$\Delta\langle\omega_\alpha\rangle = \frac{\omega_{ce}(\Delta z_e)^2 + \omega_{ch}(\Delta z_h)^2}{2\ell_\perp^2}\tan^2\theta, \tag{44}$$

where Δz_e (Δz_h) is the spread of the electron (hole) wave function along z, and ω_{ce} (ω_{ch}) is the electron (hole) cyclotron energy. For example, if $\Delta z_e = 50$ Å and $\Delta z_h = 100$ Å, tilting the field by 45° at $B_\perp = 4$ T increases the PL energy by 0.8 meV. This exceeds the change in $\langle\omega\rangle$ due to the presence of Skyrmions in the strictly 2D system (Fig. 7). A measurement of the variation of $\langle\omega\rangle$ with θ

may therefore be less suitable as a means of detecting Skyrmions in an asymmetric quantum well. However, because the subband energies are shifted *equally* on both sides of $\nu = 1$, the redshift of the LCP line remains unaffected by $B_{\|}$. The θ dependence of the redshift hence provides a means of detecting Skyrmions in an asymmetric quantum well.

In a single heterojunction the spread of the hole wave function is *different* on either side of $\nu = 1$: for $\nu < 1$ the hole is essentially free (large Δz_h), while for $\nu > 1$ the hole is confined near the electron plane (smaller Δz_h) due to the formation of an interface exciton[41]. The diamagnetic shift of the hole subband energy (HH_0) for $\nu < 1$ then differs from the diamagnetic shift for $\nu > 1$. As a result, the redshift of the LCP line acquires an additional θ dependence given by

$$\Delta\omega_- = \frac{\omega_{ch}(\Delta z_{h>})^2 - \omega_{ch}(\Delta z_{h<})^2}{2\ell_\perp^2} \tan^2\theta, \tag{45}$$

where $\Delta z_{h>}$ ($\Delta z_{h<}$) is the spread of the hole wave function for $\nu > 1$ ($\nu < 1$). Since $\Delta z_{h>} < \Delta z_{h<}$ the additional θ dependence leads to a decrease of the redshift with tilt angle, which may overwhelm the increase with tilt angle obtained for the strictly 2D system (see Fig. 8). This can explain the *decrease* of the redshift with tilt angle observed by Davies *et al.*[42] in their recent experiments on a single heterojunction. The additional θ dependence may be suppressed by applying a gate voltage to the heterojunction, which confines the hole equally on both sides of $\nu = 1$.

The application of hydrostatic pressure also causes shifts in the electron and hole subband energies due to the different pressure dependences of the GaAs and $\mathrm{Ga}_{1-x}\mathrm{Al}_x\mathrm{As}$ bandgaps. This leads to an additional pressure dependence of the PL energy which does not occur in the strictly 2D system. For an asymmetric quantum well the redshift of the LCP line remains unaffected because the subband energies are shifted equally on both sides of $\nu = 1$.

5. Optics with Skyrmions in Pure Systems

We now turn to a study of the optical properties of Skyrmions in pure systems. The initial state in a pure system is considerably different from that in a disordered system. In the absence of disorder the photoexcited hole is no longer localized near a minimum in the disorder potential. Thus Eq. (9) does not provide an adequate description of the initial state in a pure system.

To get an idea of what the initial state *should* look like, consider the recombination of ordinary electrons and a holes in a pure system. The initial state in this case is the well-known magnetoexciton[43]. The magnetoexciton has a quantum number $\mathbf{P}$, which plays the role of the total momentum in a magnetic field[44]. The energy spectrum consists of a series of bands $E_{nm}(\mathbf{P})$, where n and m are the Landau-level indices of the electron and the hole, respectively[45]. For an electron and a hole in the lowest Landau level the dispersion is $E_{00}(\mathbf{P})$. Momentum conservation allows only magnetoexcitons with $\mathbf{P}$ equal to the photon wave vector to radiate. At optical frequencies the photon wave vector may be neglected. The PL spectrum is then determined by the recombination of magnetoexcitons with $\mathbf{P} = 0$.

In light of the above considerations a number of questions arise with regard to the optical properties of Skyrmions in a pure system:

- Can a Skyrmion bind with a hole to form a "Skyrmionic" exciton?
- Does such a Skyrmionic exciton have $\mathbf{P}$ as a good quantum number?
- What is the dispersion relation of a Skyrmionic exciton?
- What selection rules apply to the recombination of a Skyrmionic exciton?

Below we aim to answer these questions. We start by exposing the underlying symmetry that is responsible for the conservation of $\mathbf{P}$ in a pure system.

5.1. *Magnetic translation group*

Conserved quantum numbers are a consequence of the invariance of a system under a group of symmetry operations. A well-known example is the angular momentum quantum number m, which results from invariance under rotations about the z axis. The symmetry group associated with the quantum number $\mathbf{P}$ is the magnetic translation group[46]. Consider a particle of mass m^* and charge q in a magnetic field $\mathbf{B} = B\hat{z}$. Because the vector potential $\mathbf{A}(\mathbf{r}) = \frac{1}{2}\mathbf{B}\times\mathbf{r}$ depends on $\mathbf{r}$, the Hamiltonian $H = \frac{1}{2m^*}[-i\nabla - \frac{q}{c}\mathbf{A}(\mathbf{r})]^2$ is *not* invariant under ordinary translations $T_{\mathbf{R}} = e^{-\mathbf{R}\cdot\nabla}$. However, H *is* invariant under *magnetic* translations $M_{\mathbf{R}} = e^{-i\mathbf{R}\cdot\mathbf{P}}$, where $\mathbf{P} = -i\nabla + \frac{q}{c}\mathbf{A}(\mathbf{r})$. Using the Baker-Haussdorf theorem, the magnetic translation can be written as $M_{\mathbf{R}} = E_{\mathbf{R}}T_{\mathbf{R}}$, where $E_{\mathbf{R}} = \exp(i\frac{q}{c}\mathbf{A}(\mathbf{R})\cdot\mathbf{r})$ is a gauge transformation. The gauge transformation compensates for the shift in the argument of the vector potential due to $T_{\mathbf{R}}$.

In contrast to the ordinary translation group, the magnetic translation group is not Abelian. From the definition of $M_{\mathbf{R}}$ one can show that two successive magnetic translations satisfy the commutation relation

$$M_{\mathbf{R}}M_{\mathbf{R}'} = e^{i\frac{q}{c}\Phi}M_{\mathbf{R}'}M_{\mathbf{R}}, \tag{46}$$

where $\Phi = \mathbf{B}\cdot(\mathbf{R}\times\mathbf{R}')$ is the flux enclosed by the parallellogram subtended by $\mathbf{R}$ and $\mathbf{R}'$. Equation (46) lies at the heart of some remarkable phenomena exhibited by charged particles in a magnetic field, such as the Aharonov-Bohm effect[47], the Hofstadter butterfly[48], and flux quantization in superconductors[49]. Applying Eq. (46) to infinitesimal magnetic translations yields the commutation relation for the generators of the magnetic translation group:

$$[P_x, P_y] = -i\frac{qB}{c}. \tag{47}$$

Because the generators of the magnetic translation group do not commute, the energy eigenstates of a charged particle in a magnetic field can be chosen as eigenstates of *either* P_x *or* P_y (Landau gauge), or as eigenstates of $P_x^2 + P_y^2$ (circular gauge), but not as eigenstates of *both* P_x *and* P_y simultaneously. Hence $\mathbf{P}$ is not a good quantum number for a charged particle in a magnetic field.

The commutator in Eq. (47) has the opposite sign for particles of opposite charge. The x and y components of $\mathbf{P} = -i\nabla_1 - i\nabla_2 + \frac{q}{c}\mathbf{A}(\mathbf{r}_1) - \frac{q}{c}\mathbf{A}(\mathbf{r}_2)$ therefore *do* commute with each other. Hence $\mathbf{P}$ *is* a good quantum number for two particles of opposite charge in a magnetic field. This is the classic result first obtained by Gor'kov and Dzyaloshinskiĭ for an exciton in a magnetic field[44]. Gor'kov and Dzyaloshinskiĭ further showed that $\mathbf{P}$ plays the role of the total momentum of the exciton in a magnetic field. This result can be understood in a simple way by considering the exciton not as two separate particles of opposite charge, but as one composite particle of zero charge. The motion of a neutral particle is unaffected by a magnetic field. Hence the center of mass of the exciton moves as a free particle whose energy eigenstates can be characterized by the total momentum $\mathbf{P}$. More generally it can be shown that for a system of N charges with $\sum_{i=1}^{N} q_i = 0$, the x and y components of

$$\mathbf{P} = \sum_{i=1}^{N}[-i\nabla + \frac{q_i}{c}\mathbf{A}(\mathbf{r}_i)] \tag{48}$$

commute with each other. Thus the energy eigenstates of any neutral system of charges may be characterized by a conserved quantum number $\mathbf{P}$.

5.2. *Variational approach to Skyrmionic excitons*

A Skyrmionic exciton consisting of a negatively charged Skyrmion and a hole *is* a charge neutral object. The Skyrmionic exciton must therefore have $\mathbf{P}$ as a good quantum number. Below we construct a variational wave function for a Skyrmionic exciton that has a definite value of $\mathbf{P}$.

The initial state consisting of a Skyrmion and a hole localized at the origin [Eq. (9)] can be written as $|i_0\rangle = a_0^\dagger|0\rangle$, where

$$a_0^\dagger = \prod_{m=0}^{\infty}(-u_m e_{m+1\downarrow}^\dagger e_{m\uparrow} + v_m)e_{0\downarrow}^\dagger h_{0m_j}^\dagger. \tag{49}$$

This state is not an eigenstate of $\mathbf{P}$. We construct an eigenstate of $\mathbf{P}$ by analogy with the tight-binding method for constructing Bloch states (which are characterized by a wave vector $\mathbf{k}$) from localized atomic orbitals[50]. We first define a state $|i_\mathbf{R}\rangle = a_\mathbf{R}^\dagger|0\rangle$, where

$$a_\mathbf{R}^\dagger = M_\mathbf{R} a_0^\dagger M_\mathbf{R}^\dagger. \tag{50}$$

The state $|i_\mathbf{R}\rangle$ describes a Skyrmion and a hole localized at $\mathbf{R}$. In the absence of disorder the states $|i_\mathbf{R}\rangle$ are degenerate with respect to $\mathbf{R}$. In the context of the tight-binding method this corresponds to the degeneracy of atomic orbitals on different sites. We form an extended state $|i_\mathbf{P}\rangle = a_\mathbf{P}^\dagger|0\rangle$ by taking a linear superposition of localized states whose coefficients are plane waves:

$$a_\mathbf{P}^\dagger = \int d^2\mathbf{R} e^{i\mathbf{P}\cdot\mathbf{R}} a_\mathbf{R}^\dagger. \tag{51}$$

Now consider the transformation properties of $|i_{\mathbf{P}}\rangle$ under magnetic translation. Magnetic translation of an eigenstate of $\mathbf{P}$ gives back the same state multiplied by $e^{-i\mathbf{P}\cdot\mathbf{R}}$. Because magnetic translations act as an Abelian group on neutral excitations, $M_{\mathbf{R}} a^\dagger_{\mathbf{R}'} M_{\mathbf{R}} = a^\dagger_{\mathbf{R}+\mathbf{R}'}$. Using this in Eq. (51) gives

$$M_{\mathbf{R}} a^\dagger_{\mathbf{P}} M^\dagger_{\mathbf{R}} = e^{-i\mathbf{P}\cdot\mathbf{R}} a^\dagger_{\mathbf{P}}, \tag{52}$$

which shows that $|i_{\mathbf{P}}\rangle$ is an eigenstate of $\mathbf{P}$.

The state $|i_{\mathbf{P}}\rangle = a^\dagger_{\mathbf{P}}|0\rangle$ given by Eqs. (49)–(51) describes a Skyrmionic exciton with generalized total momentum $\mathbf{P}$. It has an equal probability of finding the Skyrmion and the hole anywhere in the x-y plane. Because $M_{\mathbf{R}}$ commutes with H the states $|i_{\mathbf{P}}\rangle$ with different $\mathbf{P}$ are orthogonal and uncoupled by H. The energy of the Skyrmionic exciton may be obtained by minimizing

$$E_{\mathrm{SX}}(\mathbf{P}) = \frac{\langle i_{\mathbf{P}}|H|i_{\mathbf{P}}\rangle}{\langle i_{\mathbf{P}}|i_{\mathbf{P}}\rangle}. \tag{53}$$

The values of u_m and v_m that minimize the energy will now depend on $\mathbf{P}$. For $u_m = 0$ and $v_m = 1$ we recover the magnetoexciton in the lowest Landau level[45].

5.3. *Energy of the Skyrmionic exciton*

In this section we give an outline of the calculation of $E_{\mathrm{SX}}(\mathbf{P})$ starting from Eq. (53). The numerical results of the calculation are presented in Sec. 5.4 (for $\mathbf{P} = 0$) and Sec. 5.5 (for nonzero $\mathbf{P}$).

We first calculate the denominator of Eq. (53). Using Eq. (51), the denominator can be written as

$$\langle i_{\mathbf{P}}|i_{\mathbf{P}}\rangle = S \int d^2\mathbf{R}\, e^{-i\mathbf{P}\cdot\mathbf{R}} \langle i_{\mathbf{R}}|i_0\rangle, \tag{54}$$

where S is the sample area. In the coordinate representation $|i_0\rangle$ is the product of the hole state $\phi_0^*(\mathbf{r})$ and a Slater determinant of electron orbitals $\psi_m(\mathbf{r}) = -u_m\phi_{m+1}(\mathbf{r})\chi_\downarrow + v_m\phi_m(\mathbf{r})\chi_\uparrow$, where $\chi_\downarrow$ and $\chi_\uparrow$ are spin wave functions. Similarly, $|i_{\mathbf{R}}\rangle$ is the product of the hole state $M^\dagger_{\mathbf{R}}\phi_0^*(\mathbf{r})$ and a Slater determinant of electron orbitals $M_{\mathbf{R}}\psi_m(\mathbf{r})$. The overlap between two Slater determinants is given by the determinant of the matrix of overlaps between the two sets of orbitals[51]. Hence

$$\langle i_{\mathbf{R}}|i_0\rangle = e^{-\frac{|\mathbf{R}|^2}{4}} \det|A(\mathbf{R})|, \tag{55}$$

where $A(\mathbf{R})$ is a matrix whose element $A_{mm'}(\mathbf{R})$ is the overlap between $M_{\mathbf{R}}\psi_m(\mathbf{r})$ and $\psi_{m'}(\mathbf{r})$. The factor in front of the determinant is the overlap between the hole states. Since $\chi_\downarrow$ and $\chi_\uparrow$ are orthogonal,

$$A_{mm'}(\mathbf{R}) = u_m^* u_{m'} \Delta_{m+1,m'+1}(\mathbf{R}) + v_m^* v_{m'} \Delta_{mm'}(\mathbf{R}), \tag{56}$$

where $\Delta_{mm'}(\mathbf{R})$ is the overlap between $M_{\mathbf{R}}\phi_m(\mathbf{R})$ and $\phi_{m'}(\mathbf{r})$. The matrix $\Delta(\mathbf{R})$ plays a crucial role in the calculation of the energy of the Skyrmionic exciton. Its matrix elements are given by ($\mathbf{R} = X + iY$)

$$\Delta_{mm'}(\mathbf{R}) = \begin{cases} \left(\frac{m!}{m'!}\right)^{1/2} \left(\frac{\mathbf{R}^*}{\sqrt{2}}\right)^{m'-m} e^{-\frac{|\mathbf{R}|^2}{4}} L_m^{m'-m}\left(\frac{|\mathbf{R}|^2}{2}\right) & (m' \geq m) \\ \left(\frac{m'!}{m!}\right)^{1/2} \left(-\frac{\mathbf{R}}{\sqrt{2}}\right)^{m-m'} e^{-\frac{|\mathbf{R}|^2}{4}} L_{m'}^{m-m'}\left(\frac{|\mathbf{R}|^2}{2}\right) & (m > m') \end{cases}, \tag{57}$$

where $L_m^{m'}$ is a Laguerre polynomial.

In their current form, Eqs. (55)–(57) do not provide a practical way of calculating $\langle i_\mathbf{R}|i_0\rangle$. This is because the size of the matrix $A(\mathbf{R})$ is determined by the degeneracy of the Landau level, which becomes infinite in the thermodynamic limit. However, on physical grounds we expect that $\langle i_\mathbf{R}|i_0\rangle$ should only depend on those m states for which u_m and v_m are different from 0 and 1, respectively. This is indeed the case. Setting $u_m = 0$ and $v_m = 1$ for $m \geq M$, we can rewrite Eq. (55) in terms of a matrix whose size is determined by M. The algebraic manipulations that are involved essentially amount to a particle-hole transformation, whereby the filled $\nu = 1$ state $|0\rangle$ becomes the vacuum state for spin-$\uparrow$ holes. The transformed expression *does* provide a practical way of calculating $\langle i_\mathbf{R}|i_0\rangle$. A final Fourier transform then yields $\langle i_\mathbf{P}|i_\mathbf{P}\rangle$.

Next we turn to the calculation of the numerator in Eq. (53). Using Eq. (51), the numerator can be written as

$$\langle i_\mathbf{P}|H|i_\mathbf{P}\rangle = A\int d^2\mathbf{R} e^{-i\mathbf{P}\cdot\mathbf{R}}\langle i_\mathbf{R}|H|i_0\rangle. \tag{58}$$

To evaluate $\langle i_\mathbf{R}|H|i_0\rangle$ we use Wick's theorem[52]. This theorem allows us to decompose the matrix element of a product of n creation and n annihilation operators between the states $|i_0\rangle$ and $|i_\mathbf{R}\rangle$ into a product of "propagators"

$$G_{m\sigma m'\sigma'}(\mathbf{R}) = \frac{\langle i_\mathbf{R}|e^\dagger_{m\sigma}(\mathbf{R})e_{m'\sigma'}|i_0\rangle}{\langle i_\mathbf{R}|i_0\rangle}, \tag{59}$$

where $e^\dagger_{m\sigma}(\mathbf{R})$ creates an electron of spin σ in the state $M_\mathbf{R}\phi_m(\mathbf{r})$. The "propagator" $G_{m\sigma m'\sigma'}(\mathbf{R})$ gives the probability amplitude that, if a hole is created in a state with angular momentum m' and spin σ' centered on $\mathbf{R}' = 0$, it will "propagate" to a state with angular momentum m and spin σ centered on $\mathbf{R}' = \mathbf{R}$. In the coordinate representation the "propagator" is given by the overlap between two Slater determinants with one electron missing. This overlap can be expressed[51] in terms of the minors of the determinant of $A(\mathbf{R})$. The minors in turn are related to the inverse of $A(\mathbf{R})$. We thus obtain

$$\begin{aligned} G_{m\downarrow m'\downarrow}(\mathbf{R}) &= u^*_{m-1}u^*_{m'-1}A^{-1}_{m'-1,m-1}(\mathbf{R}), & (60) \\ G_{m\uparrow m'\uparrow}(\mathbf{R}) &= v^*_m v_{m'} A^{-1}_{m'm}(\mathbf{R}), & (61) \\ G_{m\downarrow m'\uparrow}(\mathbf{R}) &= u^*_{m-1}v_{m'}A^{-1}_{m-1,m'}(\mathbf{R}), & (62) \\ G_{m\uparrow m'\downarrow}(\mathbf{R}) &= v^*_m u_{m'-1}A^{-1}_{m,m'-1}(\mathbf{R}). & (63) \end{aligned}$$

At $\mathbf{R} = 0$ we have $A^{-1}_{mm'}(0) = \delta_{mm'}$, and Eqs. (60)–(63) reduce to Eqs. (12)–(14). The matrix element of H is given by

$$\frac{\langle i_{\mathbf{R}}|H|i_0\rangle}{\langle i_{\mathbf{R}}|i_0\rangle} = \varepsilon^h_{m_j} + U^Z(\mathbf{R}) + U^H(\mathbf{R}) - U^{ex}(\mathbf{R}) - U^{sk}(\mathbf{R}) - U^{eh}(\mathbf{R}), \tag{64}$$

where $\varepsilon^h_{m_j}$ is the energy of the hole[d], and

$$\begin{aligned}
U^Z(\mathbf{R}) &= \frac{1}{2}|g_e|\mu_B B \sum_{mm'} \Delta_{mm'}(\mathbf{R})(G_{m\uparrow m'\uparrow}(\mathbf{R}) - G_{m\downarrow m'\downarrow}(\mathbf{R}) + \delta_{mm'}), && (65)\\
U^H(\mathbf{R}) &= \frac{1}{2}\sum_{mm'm''m'''} V^{ee}_{mm'm''m'''}(\mathbf{R})(G_{m\downarrow m'''\downarrow}(\mathbf{R}) + G_{m\uparrow m'''\uparrow}(\mathbf{R}) - \delta_{mm'''})\\
&\quad \times (G_{m'\downarrow m''\downarrow}(\mathbf{R}) + G_{m'\uparrow m''\uparrow}(\mathbf{R}) - \delta_{m'm''}), && (66)\\
U^{ex}(\mathbf{R}) &= \frac{1}{2}\sum_{mm'm''m'''} V^{ee}_{mm'm''m'''}(\mathbf{R})(G_{m\downarrow m''\downarrow}(\mathbf{R})G_{m'\downarrow m''\downarrow}(\mathbf{R})\\
&\quad + G_{m\uparrow m''\uparrow}(\mathbf{R})G_{m'\uparrow m'''\uparrow}(\mathbf{R}) - \delta_{mm''}\delta_{m'm'''}), && (67)\\
U^{sk}(\mathbf{R}) &= \sum_{mm'm''m'''} V^{ee}_{mm'm''-1\,m'''+1}(\mathbf{R})G_{m\downarrow m''-1\,\uparrow}(\mathbf{R})G_{m'\uparrow m'''+1\,\downarrow}(\mathbf{R}), && (68)\\
U^{eh}(\mathbf{R}) &= \sum_{mm'} V^{eh}_{m00m'}(\mathbf{R})(G_{m\downarrow m'\downarrow}(\mathbf{R}) + G_{m\uparrow m'\uparrow}(\mathbf{R}) - \delta_{mm'}), && (69)
\end{aligned}$$

with

$$\begin{aligned}
V^{ee}_{mm'm''m'''}(\mathbf{R}) &= \sum_{nn'} V^{ee}_{nn'm''m'''}\Delta_{mn}(\mathbf{R})\Delta_{m'n'}(\mathbf{R}), && (70)\\
V^{eh}_{mm'm''m'''}(\mathbf{R}) &= \sum_{nn'} V^{eh}_{nn'm''m'''}\Delta_{mn}(\mathbf{R})\Delta^*_{m'n'}(\mathbf{R}). && (71)
\end{aligned}$$

One may check that at $\mathbf{R} = 0$ each of the terms in Eqs. (65)–(69) reduces to the corresponding term in Eqs. (16)–(20). After a suitable particle-hole transformation [see the discussion after Eq. (57)], Eqs. (64)–(71) provide a practical (though cumbersome) way of calculating $\langle i_{\mathbf{R}}|H|i_0\rangle$. Taking the Fourier transform yields $\langle i_{\mathbf{P}}|H|i_{\mathbf{P}}\rangle$. The calculation is completed by numerically minimizing $E_{\mathrm{SX}}(\mathbf{P})$ as a function of the parameters u_m and v_m with $m < M$.

5.4. *Zero-momentum state*

The initial state with $\mathbf{P} = 0$ is of particular interest because it is the state that determines the recombination spectrum in a disorderless system. Figure 9(a) shows the difference between the energy of a Skyrmionic exciton with $\mathbf{P} = 0$ and the energy of a magnetoexciton with $\mathbf{P} = 0$. Figure 9(b) shows the corresponding difference in spin. Figure 9 should be compared with the equivalent Fig. 6 for a Skyrmion bound to a localized hole. The two figures are very similar in their physical trends. The size of the Skyrmion bound to the itinerant hole is determined by the same three competing effects that determine the size of the Skyrmion bound to the localized hole (Sec. 4.3). Again the Skyrmion shrinks with increasing Zeeman energy, and when the hole is brought closer to the electron plane. The threshold value of g below which Skyrmions form at a given d is almost the same in both figures.

---

[d] Since in the absence of disorder $\varepsilon^h_{mm_j}$ is degenerate with respect to m we have dropped this index.

The energy and spin differences shown in Fig. 9 were obtained using a variational wave function with $M = 14$ parameters. This accounts for the discrepancy between the energy scales in Fig. 9 and Fig. 6 (which was obtained using a wave function with $M = 60$ parameters). In Fig. 10 we compare the energy and spin differences for the delocalized state $|i_{\mathbf{P}=0}\rangle$ with the energy and spin differences for the localized state $|i_{\mathbf{R}=0}\rangle$, using the *same* number of parameters ($M = 14$) for both states. Ideally we would like to use as many parameters ($M = 60$) for the delocalized state as for the localized state. Unfortunately the increased complexity of the calculation limits us at present to a maximum of $M = 14$ parameters. We believe that this number of parameters is sufficient to capture the essential features. We have found that increasing the number of parameters from $M = 10$ to $M = 14$ increases the absolute value of ΔE and ΔS_z, but does not alter their behaviour with g and d. We therefore expect that the results of a calculation with $M = 60$ parameters will be similar to those shown in Fig. 9, except for a change of scale along the vertical axes. Figure 10 demonstrates that for wave functions with the same number of parameters, the delocalized state has a lower energy and a larger spin than the localized state. From our results for the localized state using $M = 60$ parameters (Fig. 6) we therefore expect Skyrmionic excitons with at least 3–4 spin flips in systems of experimental interest.

Most importantly, our calculation shows that the lowest-energy state probed by a PL experiment at $\nu = 1$ is *not* a $\mathbf{P} = 0$ magnetoexciton. Instead, the lowest-energy state is a $\mathbf{P} = 0$ Skyrmionic exciton. In the following section we explore the consequences of this result for the optical recombination spectrum.

5.5. *Optical recombination of Skyrmionic excitons*

The selection rules for the optical recombination in a pure system require the conservation of the total generalized momentum $\mathbf{P}$. The conservation of $\mathbf{P}$ arises from the invariance of the pure system under magnetic translation, and is not required in the disordered system. In addition we still have the spin selection rule, which stipulates that the final state must contain $|S_z + \frac{1}{2}|$ reversed spins in the case of RCP recombination, and $|S_z - \frac{1}{2}|$ reversed spins in the case of LCP recombination. The reversed spins in the pure system are not simple spin flips, but spin waves which have their own momentum quantum number $\mathbf{P}$.

The selection rules allow us to make an important observation about the recombination spectrum without having to calculate the detailed line shape. Assuming (as usual) complete energy relaxation before recombination, the initial state is a Skyrmionic exciton with $\mathbf{P} = 0$ and spin S_z. The selection rules then require a final state containing $|S_z \pm \frac{1}{2}|$ spin waves, whose *total* generalized momentum is $\mathbf{P} = 0$.

For final states containing multiple spin waves, the final state energies form a continuum between $(E_f)_{min} = |S_z \pm \frac{1}{2}||g_e|\mu_B B$ (corresponding to $|S_z \pm \frac{1}{2}|$ spin waves, *each* of zero momentum), and $(E_f)_{max} = |S_z \pm \frac{1}{2}|(|g_e|\mu_B B + \sqrt{\pi/2}\, e^2/\epsilon\ell)$ (corresponding to $|S_z \pm \frac{1}{2}|$ widely separated spin-↓ quasielectrons and spin-↑ quasiholes). Here we have used Larmor's theorem, which says that the energy of a spin wave of zero momentum is given by $|g_e|\mu_B B$, regardless of the interaction among the electrons. Hence the RCP and LCP lines have an *intrinsic* width $|S_z \pm \frac{1}{2}|\sqrt{\pi/2}\, e^2/\epsilon\ell$, where the upper sign applies to RCP and the lower sign to LCP. The LCP line has a larger intrinsic width than the RCP line since more spin waves are left in the final state.

The intrinsic width is a unique feature of the recombination spectrum of a Skyrmionic exciton. A similar broadening of the line shape due to the formation of a spin texture has been found in the absorption spectrum of a Skyrmion bound to a charged impurity[10]. The recombination spectrum of a magnetoexciton has no intrinsic width because the final state is either the fully polarized state $|0\rangle$ (in the case of RCP), or a state containing one spin wave of zero momentum (in the case of LCP). In either case there is only one final-state energy, and hence the spectrum consists of a sharp line in both polarizations.

An additional *extrinsic* broadening of the luminescence lines can occur due to finite temperatures or the presence of a weak disorder. The extrinsic broadening of the recombination spectrum of a magnetoexciton has been examined in detail by Cooper and Chklovskii[32]. They have shown that the extrinsic broadening can account for the difference in line width of the RCP and LCP lines observed by Plentz *et al.*[26] in narrow quantum wells. The observed difference in line width is also consistent with the intrinsic broadening characteristic of Skyrmionic excitons, provided they could form in these narrow wells. In wide quantum wells both the intrinsic and the extrinsic mechanisms will contribute to the broadening of the luminescence lines. It would be interesting to study the evolution of the line width with temperature and disorder. The difference in line width should persist to low temperatures and high mobilities in wide wells, where the intrinsic mechanism dominates, but not in narrow wells, where the extrinsic mechanism operates.

The PL energies for the pure system can be calculated using the method of moments discussed in Sec. 4.4. Instead of the localized state $|i_0\rangle$, we now use the delocalized state $|i_{\mathbf{P}}\rangle$ in Eq. (27). We have calculated the energies of the RCP and LCP lines for transitions from the $\mathbf{P} = 0$ state. The results are qualitatively similar to the results for the disordered system shown in Fig. 7. The mean luminescence energy $\langle\omega\rangle$ increases with g up to a threshold g_c. Above the threshold $\langle\omega\rangle$ does not vary with g. By setting $u_m = 0$ and $v_m = 1$ we can show that for a magnetoexciton $\langle\omega\rangle$ is independent of g. Hence a measurement of the g dependence of $\langle\omega\rangle$ could be used to distinguish the optical recombination of a Skyrmionic exciton from the optical recombination of a magnetoexciton. However, due to the finite-size effect (Sec. 4.7) the g dependence of the redshift of the LCP line might provide a clearer optical signature. For a Skyrmionic exciton the redshift increases with g while for a magnetoexciton the redshift is independent of g. Using a wave function with $M = 14$ parameters, we find that the redshift increases by 0.03 $e^2/\epsilon\ell$ when g varies between 0.025 and 0.02 (here $d = 3\ell$). The change in the redshift may be measured by the methods discussed in Sec. 4.6.

5.6. *Dispersion relation*

Thus far our discussion has focused on the state with $\mathbf{P} = 0$, which determines the PL spectrum of the pure system at low temperatures. States with nonzero $\mathbf{P}$ can also be probed, for example by means of a resonant light scattering experiment. In this section we derive exact results for the electric dipole moment and the asymptotic form of the dispersion of a Skyrmionic exciton. We also discuss features of the dispersion relation obtained from the variational state $|i_{\mathbf{P}}\rangle$.

The electric dipole moment of a Skyrmionic exciton is given by

$$\mathbf{d} = \frac{c}{B^2}\mathbf{P} \times \mathbf{B}. \tag{72}$$

The electric dipole moment is independent of the spin, and equal to the dipole moment of a magnetoexciton in the lowest Landau level[45]. Equation (72) is a general result for a Skyrmionic exciton restricted to the lowest Landau level, which does not rely on the specific form of the variational wave function in Eqs. (49)–(51). To prove Eq. (72), we write the Gor'kov momentum for N charges in a magnetic field as

$$\mathbf{P} = \sum_{i=1}^{N} \mathbf{\Pi}_i + \frac{1}{c}\mathbf{B} \times \mathbf{d}, \tag{73}$$

where $\mathbf{\Pi}_i = -i\nabla_i - \frac{q_i}{c}\mathbf{A}(\mathbf{r}_i)$ is the dynamical momentum of charge i, and $\mathbf{d} = \sum_{i=1}^{N} q_i \mathbf{r}_i$ is the electric dipole moment. The quantities $\mathbf{P}$, $\mathbf{\Pi}_i$, and $\mathbf{d}$ should at this stage be regarded as operators. We now take the expectation value of Eq. (73) in an eigenstate of the operator $\mathbf{P}$. For a state in the lowest Landau level the expectation value of $\sum_{i=1}^{N} \mathbf{\Pi}_i$ is equal to zero. Hence $\mathbf{P} = \frac{1}{c}\mathbf{B} \times \mathbf{d}$, where $\mathbf{P}$ and $\mathbf{d}$ are now the expectation values of the corresponding operators. Taking the cross product with $\mathbf{B}$ proves Eq. (72).

We can use Eq. (72) to establish the exact asymptotic behaviour of the dispersion relation for a Skyrmionic exciton in the limit $|\mathbf{P}| \to \infty$. Suppose that, instead of Eq. (5), we were given the *exact* ground state for a Skyrmion localized at the origin of the x-y plane. Such an exact ground state has been found explicitly for the case of a hard-core interaction among the electrons[12]. We denote the exact ground state by $s_0^\dagger|0\rangle$, and its energy by $\varepsilon_{\mathrm{SK}}$. We now use the state $a_0^\dagger|0\rangle = s_0^\dagger h_{0m_j}^\dagger|0\rangle$ to construct the Skyrmionic exciton, instead of Eq. (49). The resulting state $|i_{\mathbf{P}}\rangle$ is an exact eigenstate of $H^e + H^h + V^{ee}$ with eigenvalue $\varepsilon_{m_j}^h + \varepsilon_{\mathrm{SK}}$. If $s_0^\dagger|0\rangle$ is within the lowest Landau level, $|i_{\mathbf{P}}\rangle$ has an electric dipole moment given by Eq. (72). The electric dipole moment may have two contributions: one from the separation between the hole and the center of mass of the Skyrmion, and one from the internal dipole moment of the Skyrmion relative to its center of mass. However, because the

Skyrmion is in its ground state the internal dipole moment must vanish. Hence the separation between the hole and center of mass of the Skyrmion in the state $|i_{\mathbf{P}}\rangle$ is $\mathbf{r}_0 = \mathbf{d}/e$. The electron-hole interaction V^{eh} breaks the degeneracy of the states $|i_{\mathbf{P}}\rangle$ with respect to $\mathbf{P}$. For large $|\mathbf{P}|$ the energy shift due to V^{eh} is $-e^2/(\epsilon|\mathbf{r}_0|)$. Thus the exact asymptotic behaviour of the dispersion in the limit $|\mathbf{P}| \to \infty$ is

$$E_{\mathrm{SX}}(\mathbf{P}) \sim \varepsilon^h_{m_j} + \varepsilon_{\mathrm{SK}} - \frac{e^2}{\epsilon|\mathbf{P}|\ell^2} \tag{74}$$

An approximate dispersion law for the Skyrmionic exciton is obtained by minimizing the energy of the variational state given by Eqs. (49)–(51) as a function of $\mathbf{P}$. The results for a variational state with $M = 10$ parameters are shown in Fig. 11. Near $\mathbf{P} = 0$ the dispersion is parabolic with an effective mass that differs by less than 7 % from the effective mass of a magnetoexciton. As $|\mathbf{P}|$ increases, the energy of the Skyrmionic exciton approaches that of a magnetoexciton. Above a certain value of $|\mathbf{P}|$ (approximately $3.5/\ell$ for the values of g and d chosen in Fig. 11) the magnetoexciton is the lowest-energy state within the variational space.

While the variational state gives sensible results for the dispersion at small values of $|\mathbf{P}|$, this state does not adequately describe the dispersion at large $|\mathbf{P}|$. The dispersion obtained from the variational state approaches $\varepsilon^h_{m_j} + \frac{1}{2}|g_e|\mu_B B$ as $|\mathbf{P}| \to \infty$, whereas we know from Eq. (74) that the exact dispersion must approach $\varepsilon^h_{m_j} + \varepsilon_{\mathrm{SK}}$. The failure of the variational state occurs because the Skyrmion develops a large internal dipole moment at high $|\mathbf{P}|$. To illustrate this point we calculate the pair correlation function $g_{\downarrow\uparrow}(\mathbf{r})$ for the simplest variational state with $M = 1$. This state allows only one extra spin flip. The spin flip creates an additional spin-↓ electron and a spin-↑ hole. The pair correlation function $g_{\downarrow\uparrow}(\mathbf{r})$ is proportional to the probability of finding a spin-↓ electron and a spin-↑ hole separated by $\mathbf{r}$. The result is

$$2\pi g_{\downarrow\uparrow}(\mathbf{r}) = \frac{u_0^2}{u_0^2 + \frac{1}{2}v_0^2 e^{-\frac{1}{4}\mathbf{P}^2}} \left(\frac{4}{9} + \frac{2}{27}(\mathbf{r} - \frac{1}{2}\hat{z} \times \mathbf{P})^2\right) e^{-\frac{1}{3}(\mathbf{r}-\frac{1}{2}\hat{z}\times\mathbf{P})^2}. \tag{75}$$

The average separation between the spin-↓ electrons and the spin-↑ hole is

$$\mathbf{r}_{\downarrow\uparrow} = \frac{u_0^2}{2u_0^2 + v_0^2 e^{-\frac{1}{4}\mathbf{P}^2}}\, \hat{z} \times \mathbf{P}. \tag{76}$$

For comparison, the pair correlation function for the localized Skyrmion is

$$2\pi g_{\downarrow\uparrow}(\mathbf{r}) = u_0^2 \left(\frac{3}{4} + \frac{1}{16}\mathbf{r}^2\right) e^{-\frac{1}{4}\mathbf{r}^2}, \tag{77}$$

and $\mathbf{r}_{\downarrow\uparrow} = 0$. Equation (76) shows that the average separation between the spin-↓ electrons and the spin-↑ hole becomes larger as $|\mathbf{P}|$ is increased. Thus the Skyrmion develops an internal dipole moment.

The internal dipole moment which is associated with flipping an extra spin in the state $|i_{\mathbf{P}}\rangle$ becomes energetically unfavorable at high $|\mathbf{P}|$. Hence the magnetoexciton becomes the lowest-energy state above a certain value of $|\mathbf{P}|$. According to the arguments given earlier, the internal dipole moment must vanish in the exact state $|i_{\mathbf{P}}\rangle$. The variational state thus fails to reproduce the correct asymptotic behaviour of the dispersion at large $|\mathbf{P}|$. Increasing the number of variational parameters cannot suppress the internal dipole moment and thus does not remedy this failure. The construction of a variational state that *does* produce the correct dispersion in the high-$|\mathbf{P}|$ limit is left for for future research.

6. Summary

In this review we have presented a detailed investigation of the optical properties of quantum Hall Skyrmions. Skyrmions replace ordinary spin-$\frac{1}{2}$ quasiparticles as the elementary charged excitations of a quantum Hall system at filling factor $\nu = 1$ for sufficiently small Zeeman coupling. The optical recombination of Skyrmions with photoexcited holes determines the PL spectrum near $\nu = 1$ in heterojunctions and quantum wells where the electron-hole separation exceeds a critical value.

The optical recombination in a disordered system takes place between a Skyrmion and a hole localized near a minimum in the disorder potential. The PL spectrum at $\nu \geq 1$ consists of a RCP line and a LCP line whose mean energy: (1) does not depend on g for spin-$\frac{1}{2}$ quasielectrons, (2) does depend on g for Skyrmions. At $\nu < 1$ the spectrum consists of a LCP line shifted down in energy from the LCP line at $\nu \geq 1$. The g dependence of the redshift provides a way to determine the nature of the negatively charged excitations using PL spectroscopy. The redshift increases with g if the charged excitations are Skyrmions, but does not depend on g is they are spin-$\frac{1}{2}$ quasielectrons. The g dependence of the redshift can be measured, for example, by tilting the magnetic field or by applying hydrostatic pressure.

Skyrmionic excitons—consisting of a Skyrmion and a hole bound together by their mutual Coulomb attraction—govern the optical recombination in a pure system. Skyrmionic excitons replace ordinary magnetoexcitons as the lowest-energy excitations probed by a PL experiment at $\nu = 1$. The g dependence of the redshift of the LCP line can be used to distinguish between the optical recombination of a Skyrmionic exciton and the optical recombination of a magnetoexciton. Skyrmionic excitons have their own dispersion relation in terms of a quantum number $\mathbf{P}$, which plays the role of the total momentum in a magnetic field. The electric dipole moment of a Skyrmionic exciton is independent of its spin and equal to the dipole moment of a magnetoexciton.

It is hoped that the results presented in this review will aid in the interpretation of PL experiments on quantum Hall systems near filling factor $\nu = 1$. They might also be of relevance to spectroscopic studies at other filling factors for which the ground state is spin polarized. For a more detailed comparison between theory and experiment a calculation of the line shape is needed. Efforts in this direction are currently underway.

Acknowledgements

We thank Andrew Turberfield, Darren Leonard, Georg Bruun, Igor Lerner, and Stuart Trugman for helpful discussions. This work was supported by EPSRC Grant No. GR/K 15619.

Figures

Fig. 1. Spin profile of (a) a negatively charged Skyrmion, (b) a positively charged Skyrmion. (Adapted from Ref. 19.)

Fig. 2. (a) Energy, and (b) spin of a negatively charged Skyrmion as a function of $g = \frac{1}{2}|g_e|\mu_B B/(e^2/\epsilon\ell)$. Dash-dotted line: energy of a spin-$\frac{1}{2}$ quasielectron.

Fig. 3. Band diagram of a one-side modulation-doped quantum well. The lowest electron (E_0) and hole (HH_0) energy levels and z wave functions are shown. Dotted lines indicate the average positions of electrons and holes along z.

Fig. 4. Magnetic-field dependence of the E_0 luminescence energy from a GaAs/Ga$_{0.68}$Al$_{0.32}$As heterojunction with electron density $n_s = 9.7 \times 10^{10}$ cm^{-2} and mobility $\mu = 9 \times 10^6$ cm^{2}V^{-1}s^{-1} at $T = 120$ mK. Inset shows the luminescence spectra at selected magnetic fields. (Reprinted with kind permission from Andrew Turberfield.)

Fig. 5. Comparison of PL at $\nu = 1$ (left column) and $\nu = 1^-$ (right column). (a) Ground state before photoexcitation. (b) Initial state before recombination. (c) Final state after LCP recombination. (d) Final state after RCP recombination.

Fig. 6. Difference in (a) energy and (b) spin between an initial state consisting of a Skyrmion and a localized hole, and an initial state consisting of a spin-$\downarrow$ electron and a localized hole against a $\nu = 1$ background.

Fig. 7. Mean luminescence energy $\langle\omega\rangle$ as a function of g, for several values of the separation d between the electron and hole planes. Remaining parameter values are for a GaAs/Ga$_{1-x}$Al$_x$As heterojunction with electron density $n_s = 10^{11}$ cm^{-2}. The gap value $E_g = 1509$ meV was taken from Ref. 21.

Fig. 8. Variation of the redshift of the LCP line with tilting angle (θ) and applied hydrostatic pressure (p) for a GaAs/Ga$_{1-x}$Al$_x$As quantum well or heterojunction with $n_s = 10^{11}$ cm^{-2} and a separation of $d = 400$ Å between the electron and hole planes.

Fig. 9. Difference in (a) energy and (b) spin between a Skyrmionic exciton with $\mathbf{P} = 0$ and a magnetoexciton with $\mathbf{P} = 0$. The energy and spin are plotted as a function of the reduced Zeeman energy g, for several values of the separation d between the electron and hole planes. The number of variational parameters is $M = 14$.

Fig. 10. Comparison of (a) energy and (b) spin differences for the delocalized state $|i_{\mathbf{P}=0}\rangle$ and the localized state $|i_{\mathbf{R}=0}\rangle$. The energy and spin differences were calculated using the same number of variational parameters ($M = 14$) for both the delocalized and the localized state. The separation between the electron and hole planes is $d = 3\ell$.

Fig. 11. Solid line: dispersion relation for the Skyrmionic exciton (SX) obtained from a variational state with $M = 10$ parameters. Dash-dotted line: dispersion relation for a magnetoexciton (MX) in the lowest Landau level. $g = 0.005$ and $d = 3\ell$.

References

1. T. H. R. Skyrme, *Proc. R. Soc. London Ser. A:* **247**, 260 (1958).
2. S. L. Sondhi, A. Karlhede, S. A. Kivelson, and E. H. Rezayi, *Phys. Rev. B* **47**, 16419 (1994).
3. D. H. Lee and C. L. Kane, *Phys. Rev. Lett.* **64**, 1313 (1990).
4. S. E. Barrett, G. Dabbagh, L. N. Pfeiffer, K. W. West, and R. Tycko, *Phys. Rev. Lett.* **74**, 5112 (1995).
5. A. Schmeller, J. P. Eisenstein, L. N. Pfeiffer, and K. W. West, *Phys. Rev. Lett.* **75**, 4290 (1995).
6. E. H. Aifer, B. B. Goldberg, and D. A. Broido, *Phys. Rev. Lett.* **75**, 4290 (1995).
7. D. K. Maude *et al.*, *Phys. Rev. Lett.* **77**, 4604 (1996).
8. H. A. Fertig, L. Brey, R. Côté, and A. H. MacDonald, *Phys. Rev. B* **50**, 11018 (1994).
9. L. Brey, H. A. Fertig, R. Côté, and A. H. MacDonald, *Phys. Rev. Lett.* **75**, 2562 (1995).
10. H. A. Fertig, L. Brey, R. Côté, and A. H. MacDonald, *Phys. Rev. Lett.* **77**, 1572 (1996).
11. A. G. Green, I. I. Kogan, and A. M. Tsvelik, *Phys. Rev. B* **54**, 16838 (1996).
12. A. H. MacDonald, H. A. Fertig, and L. Brey, *Phys. Rev. Lett.* **76**, 2153 (1996).
13. Yu. A. Bychkov, T. Maniv, and I. D. Vagner, *Phys. Rev. B* **53**, 10148 (1996).
14. X. C. Xie and S. He, *Phys. Rev. B* **53**, 1046 (1996).
15. R. K. Kamilla, X. G. Wu, and J. K. Jain, *Solid State Commun.* **99**, 283 (1996).
16. K. H. Ahn and K. J. Chang, *Phys. Rev. B* **55**, 6735 (1997).
17. T. Portengen, J. R. Chapman, V. Nikos Nicopoulos, and N. F. Johnson, *Phys. Rev. B* **55**, R7367 (1997).
18. T. Portengen, J. R. Chapman, V. Nikos Nicopoulos, and N. F. Johnson, *to appear in Phys. Rev. B.*
19. see, for example, T. Chakraborty and P. Pietiläinen, *The Fractional Quantum Hall Effect* (Springer, Berlin, 1988), Appendix A.
20. R. B. Laughlin, in *The Quantum Hall Effect*, ed. R. E. Prange and S. M. Girvin (Springer, Berlin, 1987), p. 260.
21. *Phys. Today*, July 1995, p. 19.
22. J. R. Schrieffer, *Theory of Superconductivity*, 4th ed. (Addison-Wesley, Redwood City, CA, 1988).
23. A. J. Turberfield *et al.*, *Phys. Rev. Lett.* **65**, 637 (1990).
24. B. B. Goldberg, D. Heiman, A. Pinczuk, L. Pfeiffer, and K. W. West, *Phys. Rev. Lett.* **65**, 641 (1990).
25. B. B. Goldberg, D. Heiman, A. Pinczuk, L. Pfeiffer, and K. W. West, *Surf. Sci.* **263**, 9 (1992).
26. F. Plentz *et al.*, in *High Magnetic Fields in the Physics of Semiconductors*, ed. D. Heiman (World Scientific, Singapore, 1995), p. 320.
27. C. Weisbuch and B. Vinter, *Quantum Semiconductor Structures* (Academic Press, San Diego, 1991).
28. H. Buhmann *et al.*, Phys. Rev. Lett. **65**, 1056 (1990).
29. H. Buhmann *et al.*, Phys. Rev. Lett. **66**, 926 (1991).
30. I. V. Kukushkin *et al.*, Phys. Rev. B **45**, 4532 (1992).
31. B. A. Muzykantskiĭ, *Zh. Eksp. Teor. Fiz.* **101**, 1084 (1992) [*Sov. Phys. JETP* **74**, 897 (1992)].
32. N. R. Cooper and D. B. Chklovskii, *Phys. Rev. B* **42**, 3224 (1996).
33. J. K. Jain, *Adv. Phys.* **41**, 105 (1992), and references therein.
34. K. Inoue, H. Sakaki, and J. Yoshino, *Jpn. J. Appl. Phys.* **23**, L767 (1984).
35. M. H. Meynadier *et al.*, *Phys. Rev. B* **34**, 2482 (1986).
36. N. M. Cho, S. B. Ogale, and A. Madhukar, *Appl. Phys. Lett.* **51**, 1016 (1987).

37. F. Yang, M. Wilkinson, E. J. Austin, and K. P. O'Donnell, *Phys. Rev. Lett.* **70**, 323 (1993).
38. V. M. Apalkov and E. I. Rashba, *Pis'ma Zh. Eksp. Teor. Fiz.* **53**, 442 (1991) [*JETP Lett.* **53**, 442 (1991)].
39. S. Holmes *et al.*, *Semicond. Sci. Technol.* **9**, 1549 (1995).
40. T. Ando, A. B. Fowler, and F. Stern, *Rev. Mod. Phys.* **54**, 438 (1982).
41. N. A. Viet and J. L. Birman, *Phys. Rev. B* **51**, 14337 (1995).
42. H. D. M. Davies *et al.*, in *Proceedings of the 12th International Conference on the Electronic Properties of Two-Dimensional Systems*, ed. H. Aoki (North-Holland, Amsterdam, 1997) (to be published).
43. For a review, see A. V. Korolev and M. A. Liberman, *Int. J. Mod. Phys. B* **10**, 729 (1996).
44. L. P. Gor'kov and I. E. Dzyaloshinskiĭ, *Zh. Eksp. Teor. Fiz.* **53**, 717 (1967) [*Sov. Phys. JETP* **26**, 449 (1968)].
45. I. V. Lerner and Yu. E. Lozovik, *Zh. Eksp. Teor. Fiz.* **78**, 1167 (1978) [*Sov. Phys. JETP* **51**, 588 (1980)].
46. J. Zak, *Phys. Rev.* **134** A 1602 (1964).
47. Y. Aharonov and D. Bohm, *Phys. Rev.* **115**, 485 (1959).
48. D. R. Hofstadter, *Phys. Rev. B* **14**, 2239 (1976).
49. C. Kittel, *Introduction to Solid State Physics*, 6th ed. (John Wiley, New York, 1986), p. 340.
50. N. W. Ashcroft and N. D. Mermin, *Solid State Physics*, (Saunders College, Philadelphia, 1976), Ch. 10.
51. P. O. Löwdin, *Phys. Rev.* **97**, 1474 (1955).
52. G. D. Mahan, *Many-Particle Physics*, 2nd ed. (Plenum, New York, 1990), Sec. 2.4.

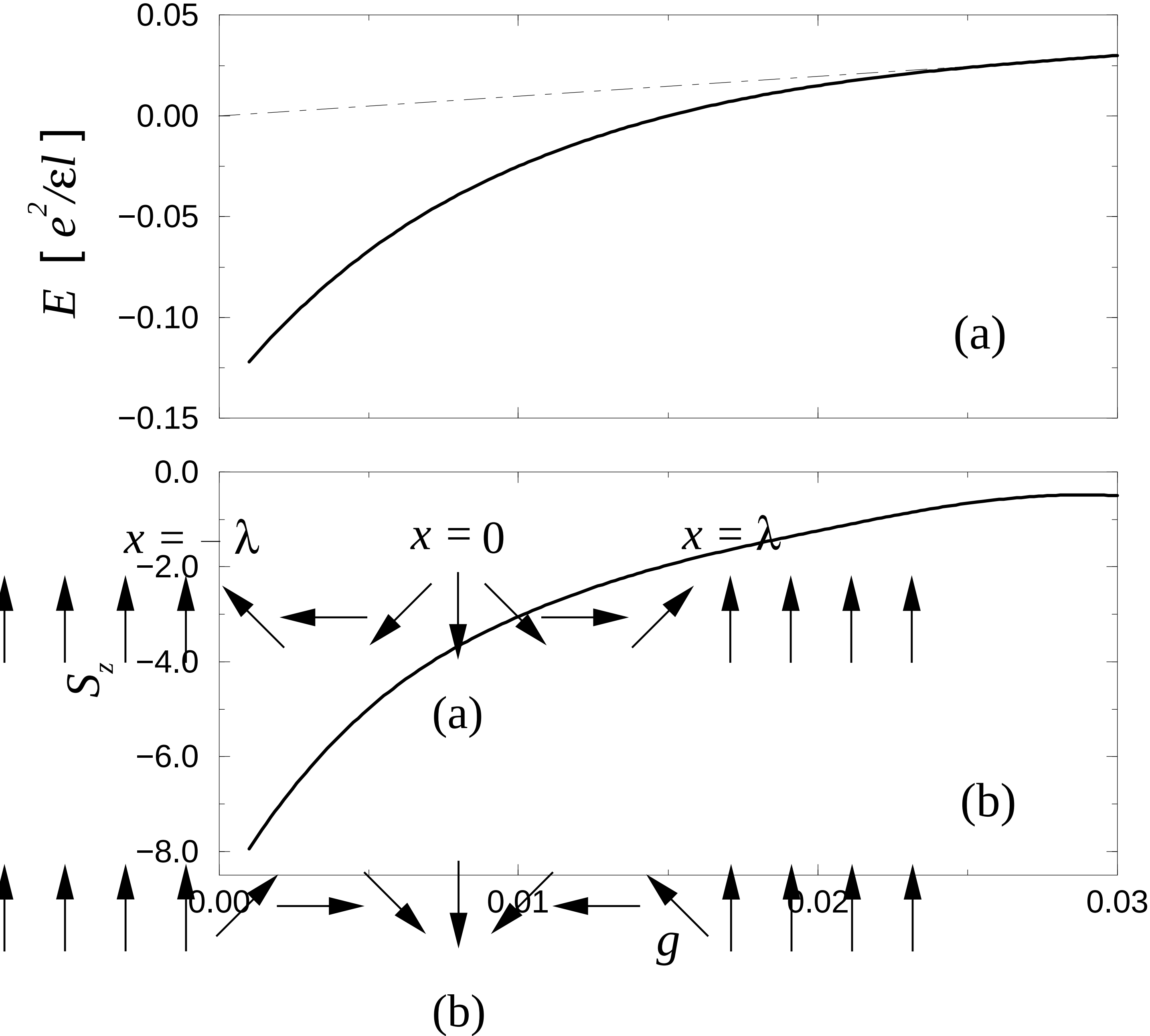
0.05
0.00
−0.05
−0.10
−0.15
E [$e^2/\varepsilon l$]
(a)
0.0
−2.0
−4.0
−6.0
−8.0
S_z
(b)
0.00
0.01
0.02
0.03
g
$x = -\lambda$
$x = 0$
$x = \lambda$
(a)
(b)

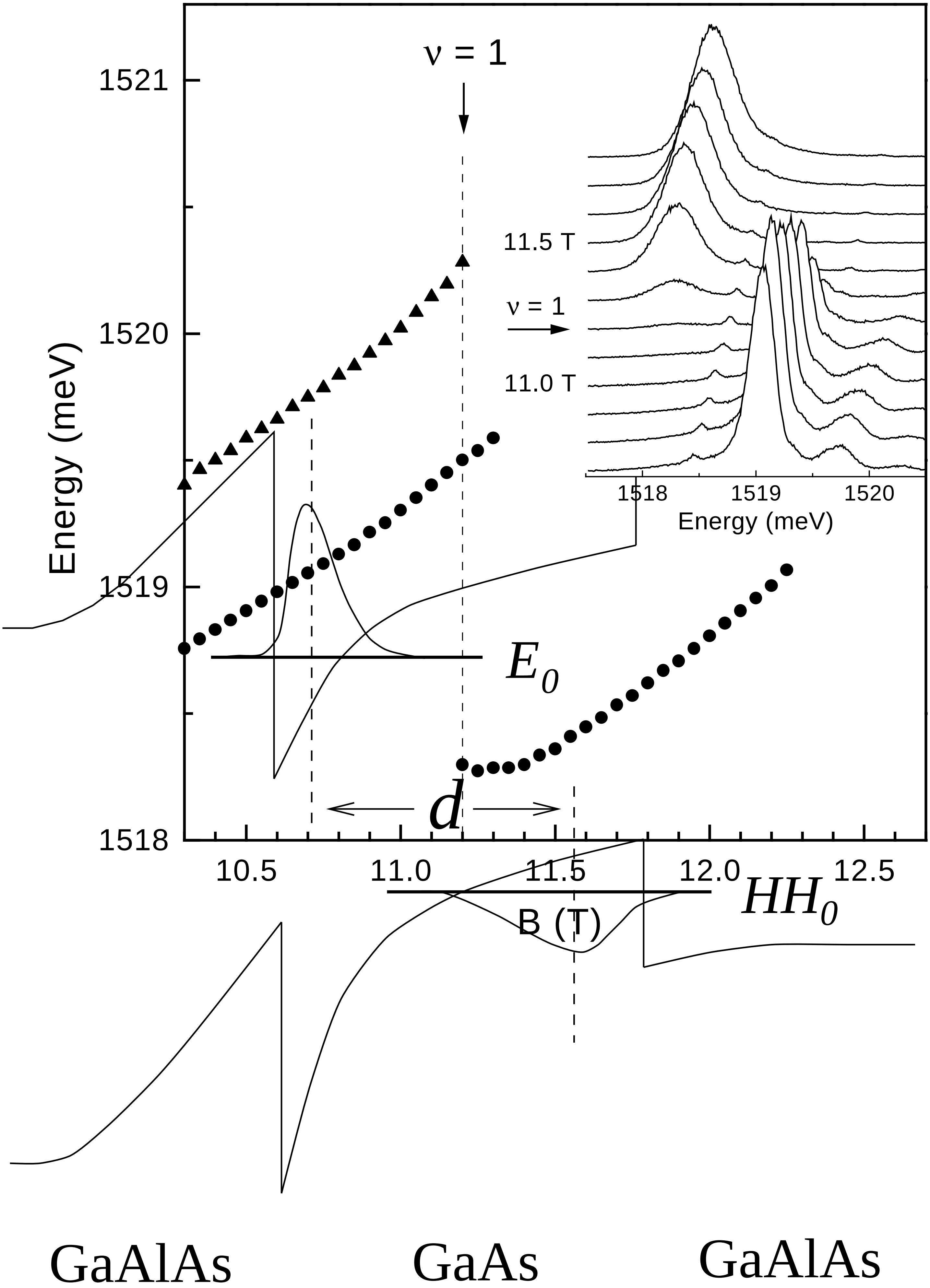
ν = 1
1521
1520
1519
1518
Energy (meV)
10.5
11.0
11.5
12.0
12.5
B (T)
E0
d
HH0
11.5 T
ν = 1
11.0 T
1518
1519
1520
Energy (meV)
GaAlAs
GaAs
GaAlAs

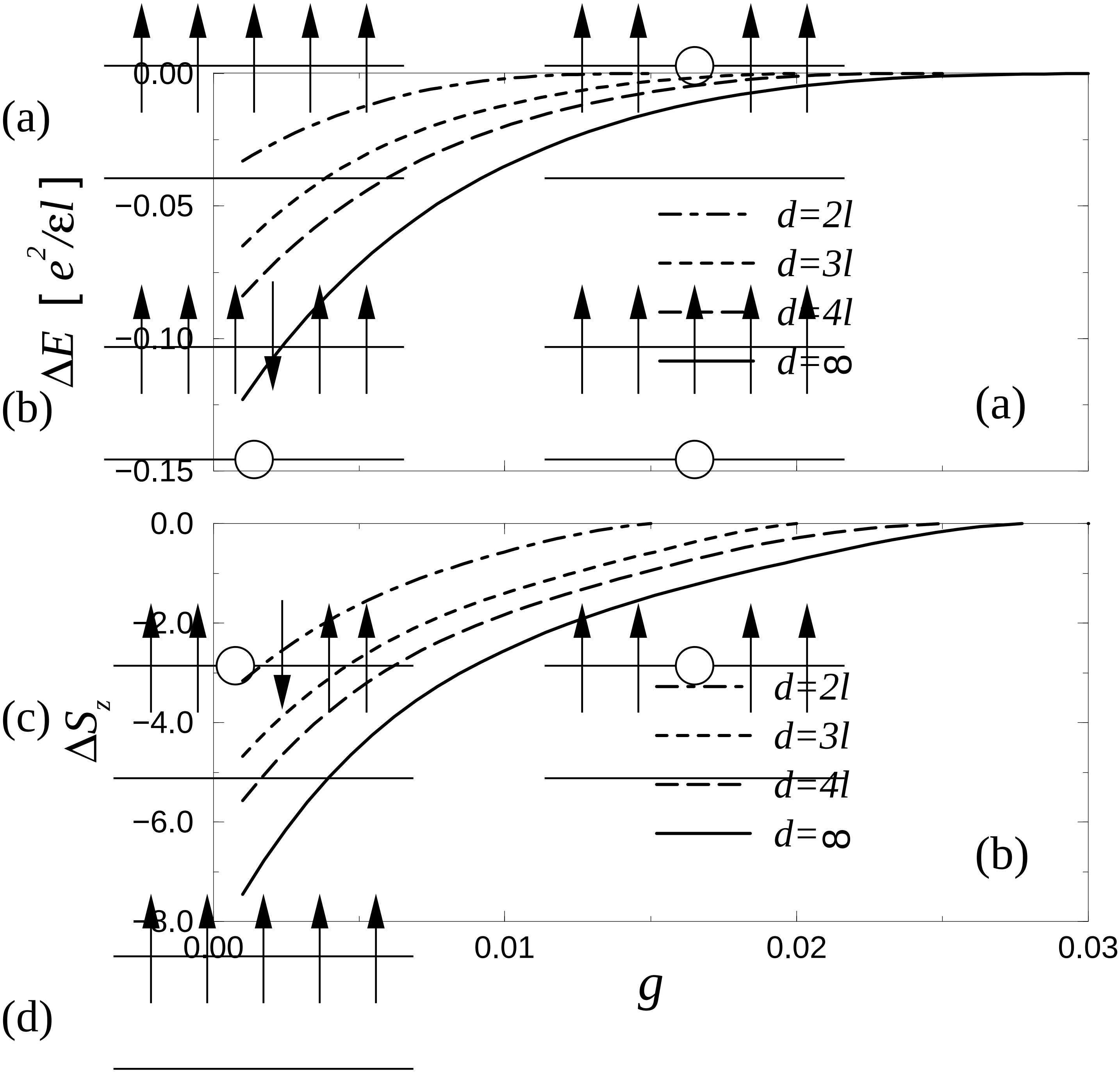
(a)
(b)
(c)
(d)
0.00
−0.05
−0.10
−0.15
ΔE [e²/εl]
d=2l
d=3l
d=4l
d=∞
(a)
0.0
−2.0
−4.0
−6.0
−8.0
ΔS_z
d=2l
d=3l
d=4l
d=∞
(b)
0.00
0.01
0.02
0.03
g

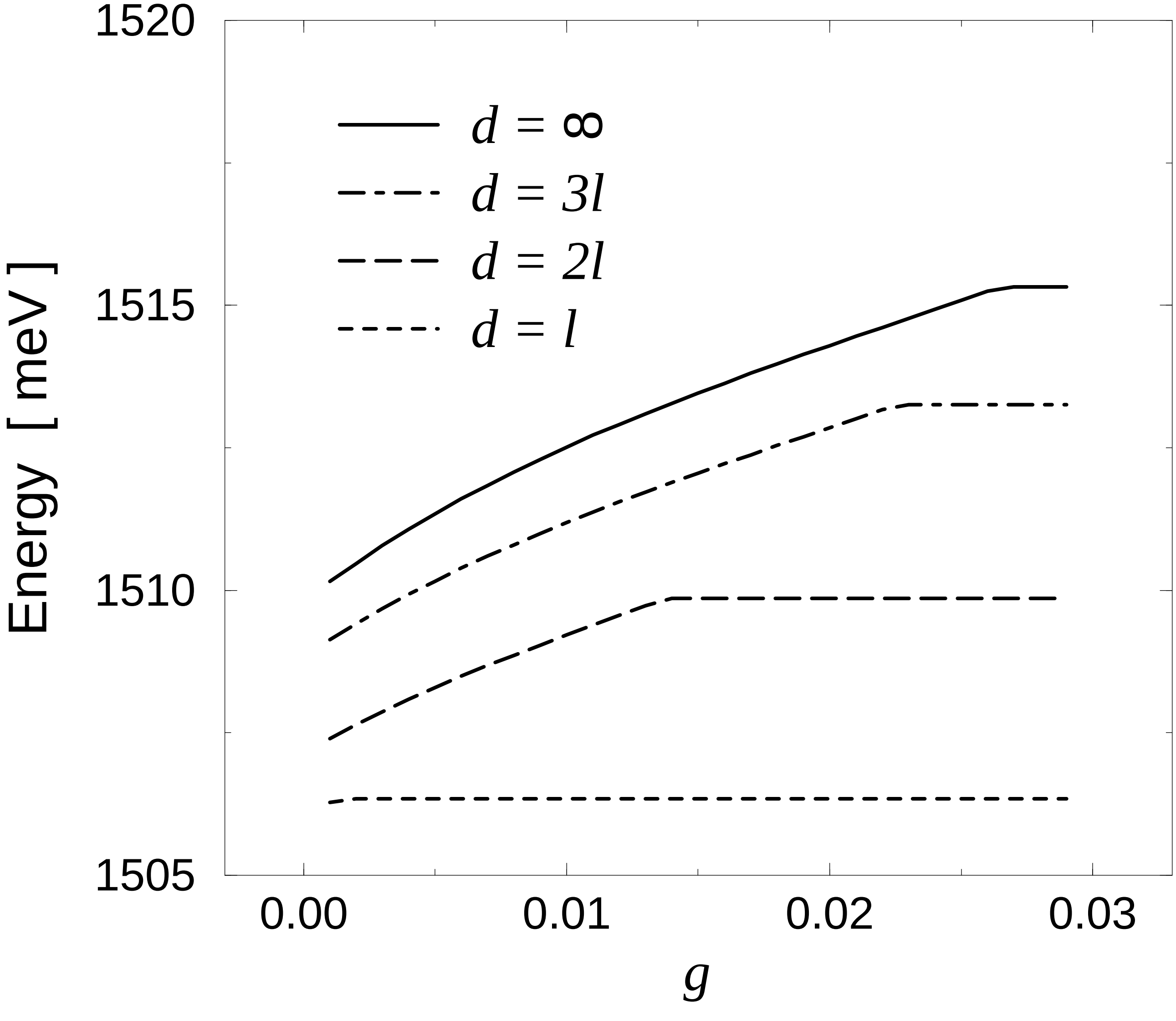
1520
1515
1510
1505
0.00
0.01
0.02
0.03
Energy [meV]
g
d = ∞
d = 3l
d = 2l
d = l

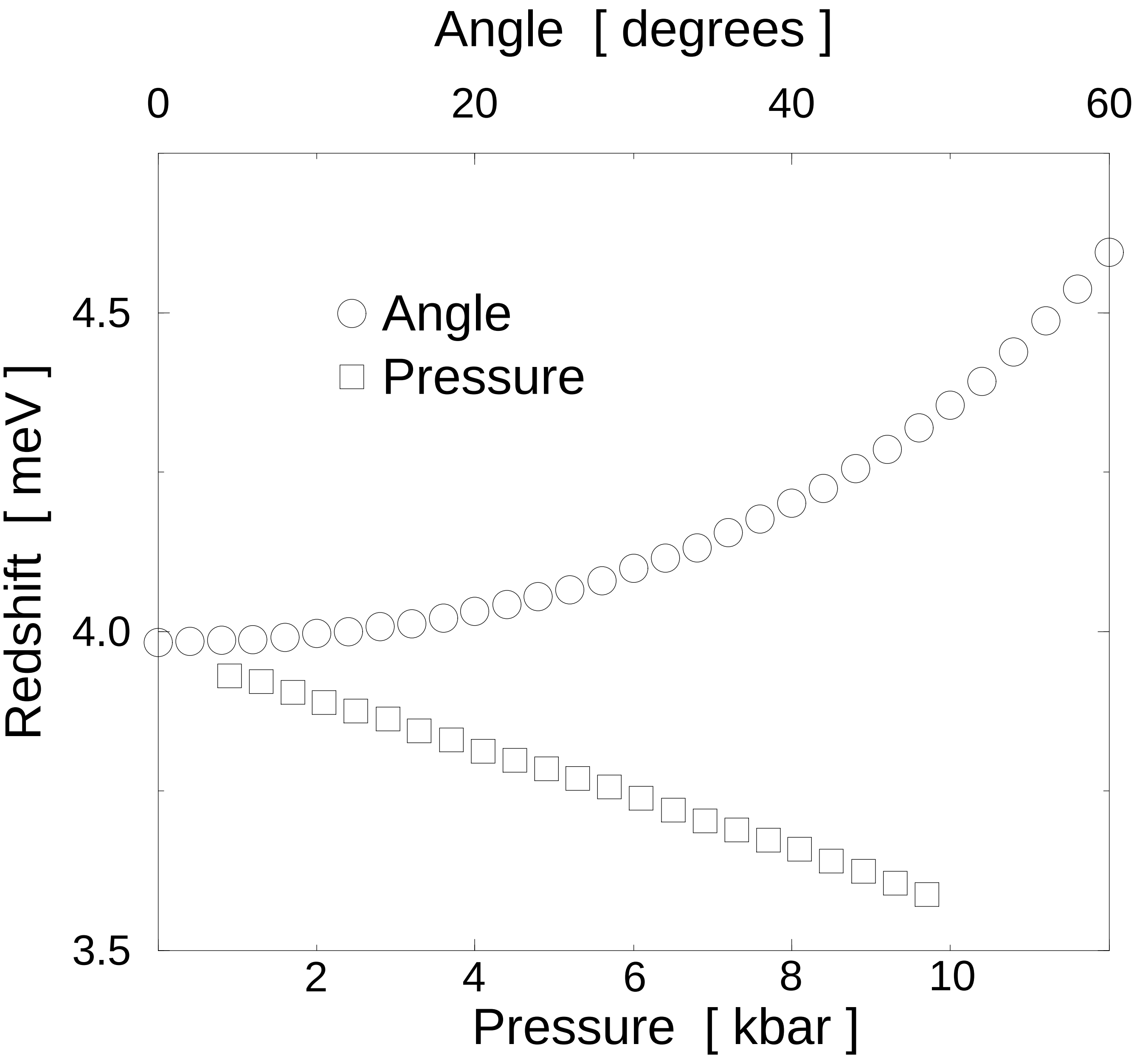
Angle [degrees]
0
20
40
60
Angle
Pressure
Redshift [meV]
4.5
4.0
3.5
2
4
6
8
10
Pressure [kbar]

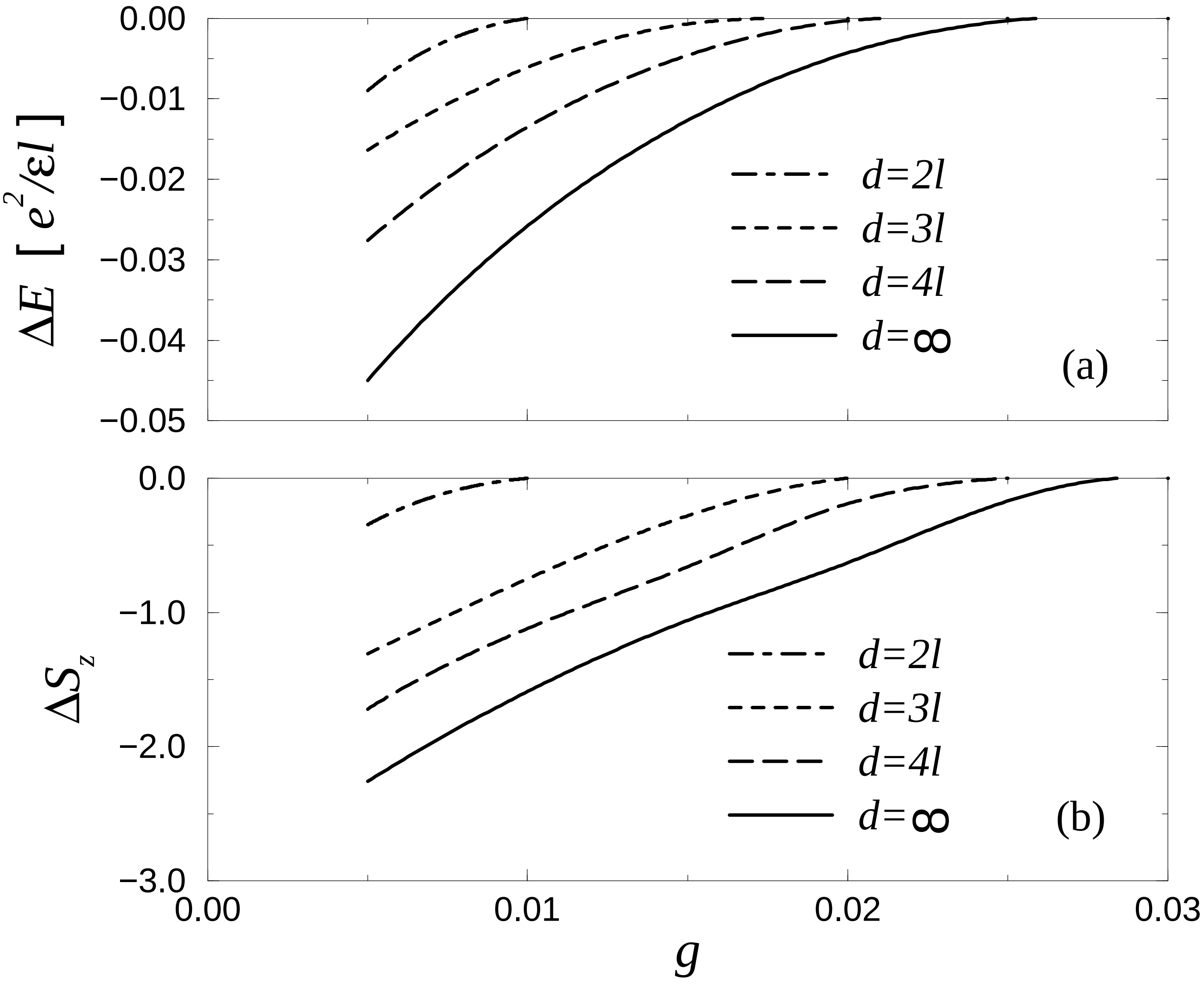

0.00
−0.01
−0.02
−0.03
−0.04
−0.05
ΔE [$e^2/\varepsilon l$]
$d=2l$
$d=3l$
$d=4l$
$d=\infty$
(a)
0.0
−1.0
−2.0
−3.0
ΔS_z
$d=2l$
$d=3l$
$d=4l$
$d=\infty$
(b)
0.00
0.01
0.02
0.03
g

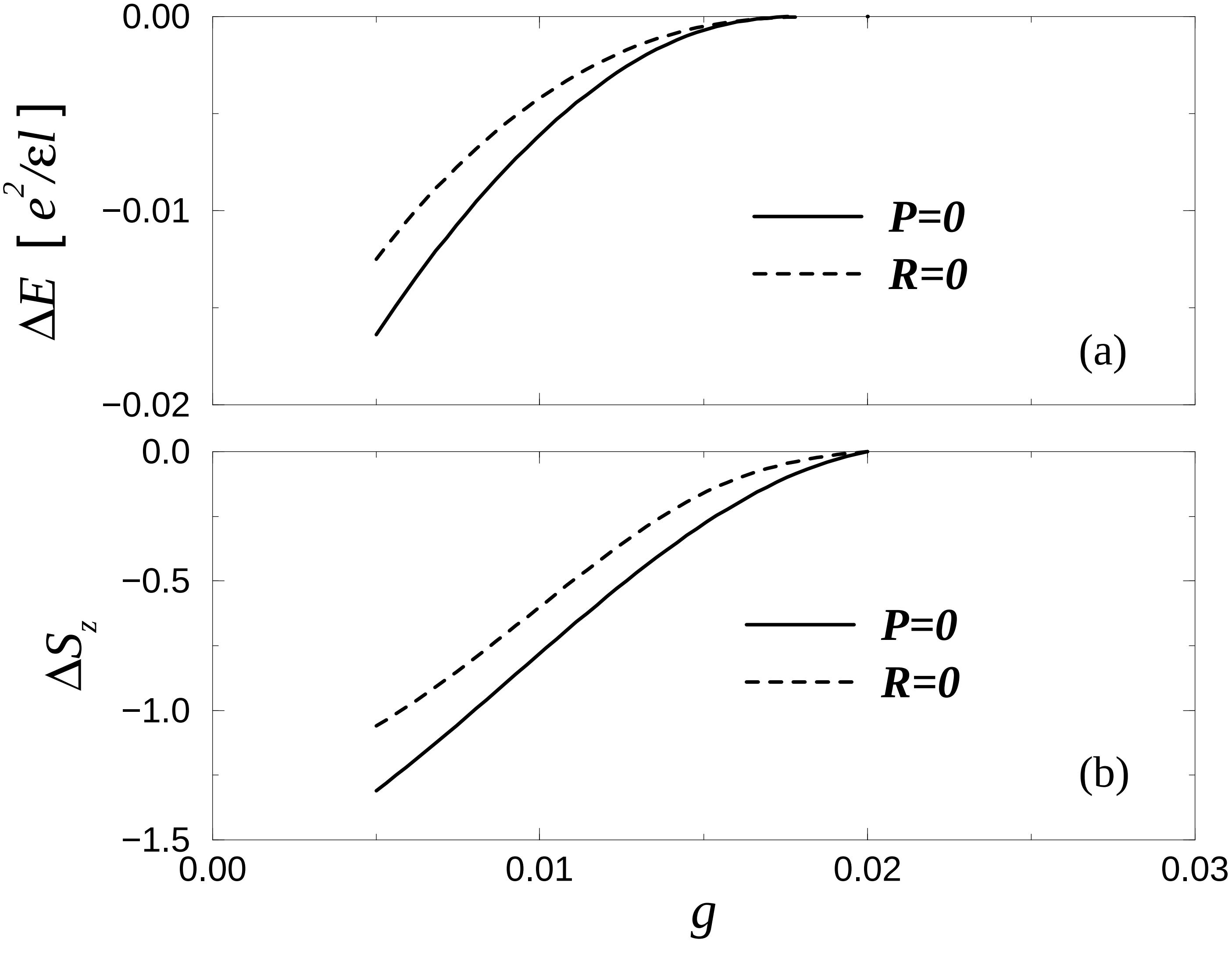

0.00
−0.01
−0.02
ΔE [e²/εl]
P=0
R=0
(a)
0.0
−0.5
−1.0
−1.5
ΔS_z
P=0
R=0
(b)
0.00
0.01
0.02
0.03
g

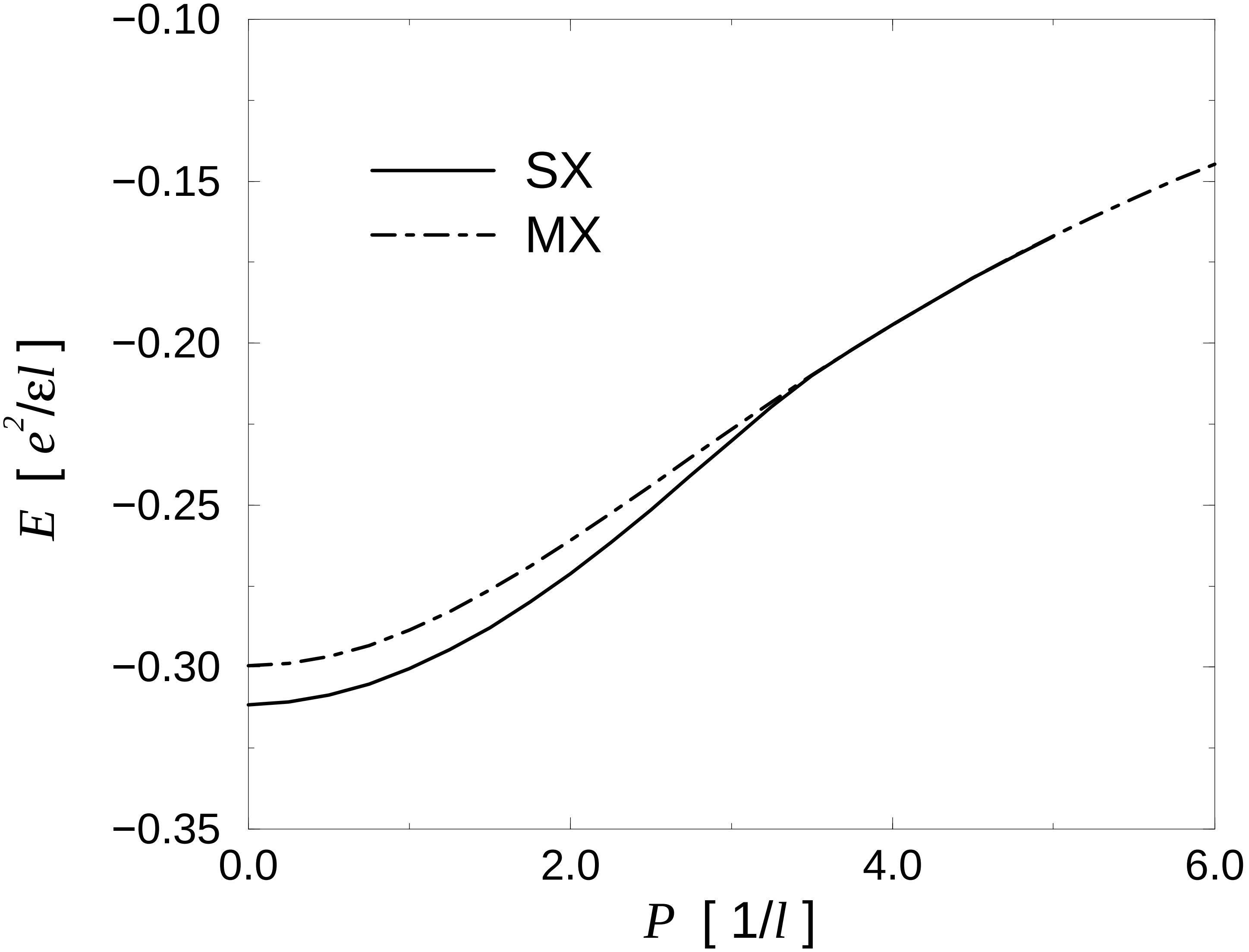

−0.10
−0.15
−0.20
−0.25
−0.30
−0.35
0.0
2.0
4.0
6.0
SX
MX
E [$e^2/\varepsilon l$]
P [$1/l$]